Journal of proteome research

Open Access

pubs.acs.org/jpr

Article

Shotgun Proteomic-Based Approach with a Q-Exactive Hybrid Quadrupole-Orbitrap High-Resolution Mass Spectrometer for Protein Adductomics on a 3D Human Brain Tumor Neurospheroid Culture Model: The Identification of Adduct Formation in Calmodulin-Dependent Protein Kinase-2 and Annexin-A1 Induced by Pesticide Mixture

Kaouthar Louati,* Amina Maalej, Fatma Kolsi, Rim Kallel, Yassine Gdoura, Mahdi Borni, Leila Sellami Hakim, Rania Zribi, Sirine Choura, Sami Sayadi, Mohamed Chamkha, Basma Mnif, Zouheir Khemakhem, Tahya Sellami Boudawara, Mohamed Zaher Boudawara, and Fathi Safta

Cite This: *J. Proteome Res.* 2023, 22, 3811−3832

Read Online

ACCESS | Metrics & More | Article Recommendations | Supporting Information

ABSTRACT: Pesticides are increasingly used in combinations in crop protection, resulting in enhanced toxicities for various organisms. Although protein adductomics is challenging, it remains a powerful bioanalytical tool to check environmental exposure and characterize xenobiotic adducts as putative toxicity biomarkers with high accuracy, facilitated by recent advances in proteomic methodologies and a mass spectrometry high-throughput technique. The present study aims to predict the potential neurotoxicity effect of imidacloprid and λ-cyhalothrin insecticides on human neural cells. Our protocol consisted first of 3D in vitro developing neurospheroids derived from human brain tumors and then treatment by pesticide mixture. Furthermore, we adopted a bottom-up proteomic-based approach using nanoflow ultraperformance liquid chromatography coupled with a high-resolution mass spectrometer for protein-adduct analysis with prediction of altered sites. Two proteins were selected, namely, calcium-calmodulin-dependent protein kinase-II (CaMK2) and annexin-A1 (ANXA1), as key targets endowed with primordial roles. *De novo* sequencing revealed several adduct formations in the active site of 82-ANXA1 and 228-CaMK2 as a result of neurotoxicity, predicted by the added mass shifts for the structure of electrophilic precursors. To the best of our knowledge, our study is the first to adopt a proteomic-based approach to investigate in depth pesticide molecular interactions and their potential to adduct proteins which play a crucial role in the neurotoxicity mechanism.

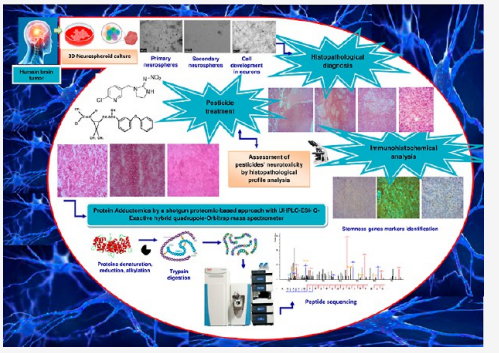

KEYWORDS: *neurospheroids, brain tumors, tandem mass spectrometry, protein adductomics, untargeted-proteomic-based approach, neurotoxicity, toxicity biomarkers, peptide sequencing*

1. INTRODUCTION

Nowadays, humans are constantly exposed to a wide range of physical stressors and environmental toxic chemicals, which may be contributing factors to human hazardous health effects. By way of illustration, pesticide mixtures are frequently used in agricultural areas to improve productivity and reduce the cost of crop pest treatment. However, their persistence and pervasiveness in the environment along with their biotransformation products ensure the presence of such combinations in foodstuffs which result in enhanced toxicities for various organisms.[1−10] Long-term occupational or nonoccupational exposure to low doses of pesticides is of great concern to the general population as they can have teratogenic, carcinogenic, oncogenic, and mutagenic effects, as well as cause other negative disorders, such as dermatological, gastrointestinal, neurological, respiratory, and endocrine effects.[11−20]

In recent years, pyrethroid and neonicotinoid insecticides have constituted the most widely used class of synthetic pesticides since restrictions have been placed on various methylcarbamate and organophosphorus insecticides due to their increased mammalian toxicity and reduced effectiveness

Received: August 3, 2023
Revised: September 27, 2023
Accepted: October 16, 2023
Published: October 31, 2023

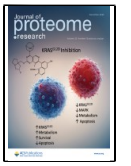

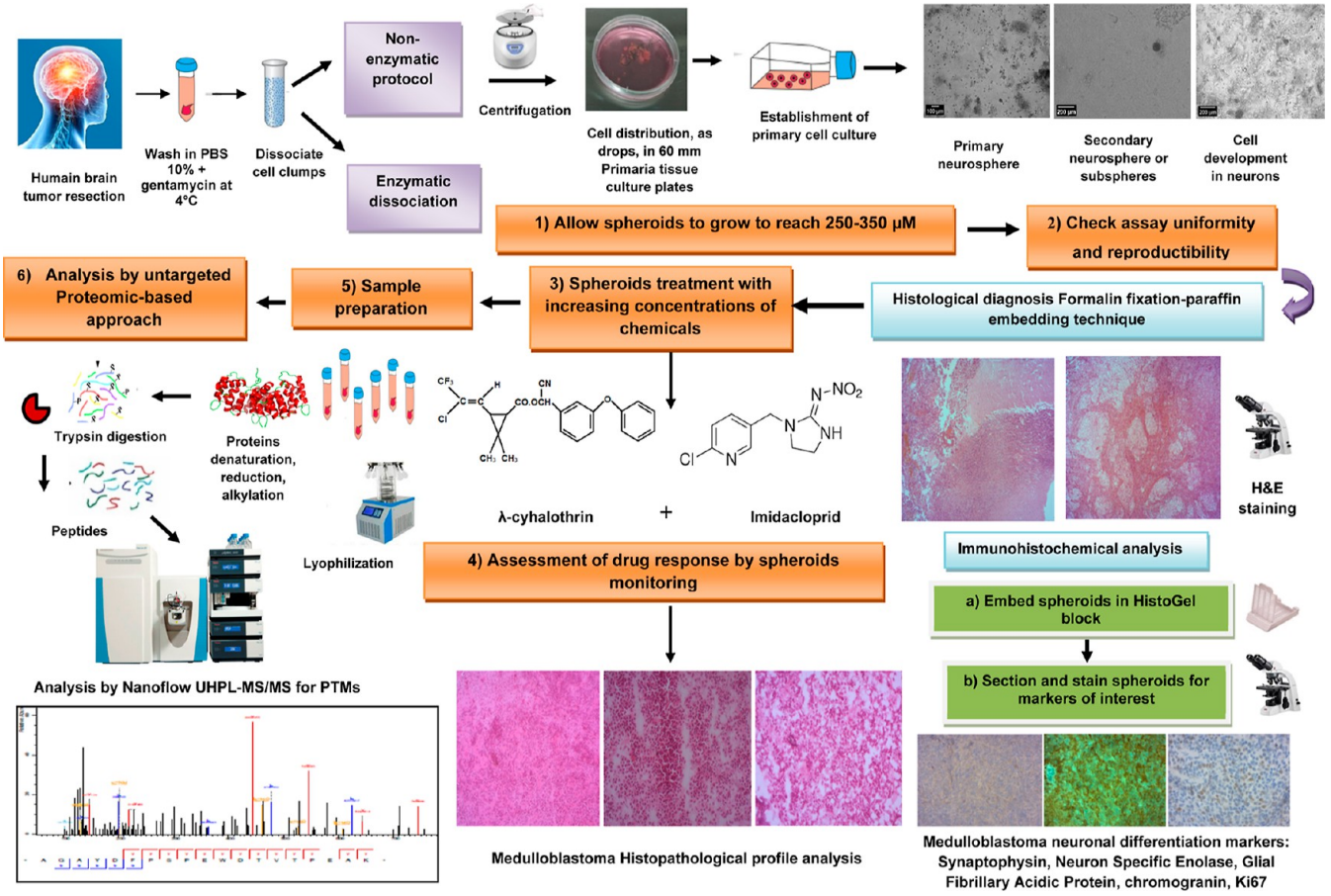

Figure 1. Schematic illustration of the full methodology by a shotgun proteomic-based approach for protein adductomics on a 3D human brain tumor neurospheroid culture model.

in pest resistance.[21,22] Lambda-cyhalothrin (λ-CYH) is a new generation type II synthetic pyrethroid, while imidacloprid (IMD) is derived from the neonicotinoid pesticide class. These two types of pesticides exhibit high-efficacy, broad-spectrum practices on a wide range of insects, including resistance strains,[23] and low toxicity to mammals and birds.[24−27] In our Tunisian market, this mixture has swiftly emerged as one of the safest and lowest-risk ones currently available in modern agricultural practices.[24−26]

Previous toxicological studies on λ-CYH and IMD were conducted on nontargeted organisms including animals (rabbits, mice, insects, and bees)[22,28−33] and aquatic creatures (fish and carps)[34,35] to either investigate the potential neurotoxic effect of each pesticide alone[28,36,37] or in combination[38−40] or assess their endocrine-disrupting activity,[41] as well as genotoxicity,[42] metabolic impairment, and oxidative damage.[37,43] However, there is a lack of studies about their possible synergistic effects on human neuronal and glial cellular systems, and the corresponding molecular mechanisms of neurotoxicity are poorly understood.

Pesticides are known to induce toxicity at the cellular level either by covalently binding macromolecules[44] or through alterations in redox homeostasis by the generation of oxidative stress following the overproduction of reactive oxygen species (ROS).[45] Proteins, one of the major targets of oxygen free radicals and other reactive species, may either encounter post-translational modification (PTM) or be modified by covalent adduct formation on its key amino acid side chains to initiate toxicity via modification of its structure and/or cellular function, which secondarily deregulates several cytological processes and/or signaling pathways,[46−49] alters tight junctions,[50,51] or damages all cell constituents including protein chaperones, DNA, and lipids, leading to apoptotic or necrotic cell death, lipid peroxidation, and metabolic perturbation.[11,52−56]

Increased knowledge about the potential modification of a target protein in a human sample by detecting and characterizing covalent adducts formed after environmental xenobiotic exposure allowed the gain of two potential benefits: first, a better understanding of the underlying mechanism involved in the toxicological condition, and second, their identification as potential predictors or prognostic biomarkers gives insights into environmental agents and endogenous processes inherent to human genetics,[46] as well as assessing toxicity outcomes and designing treatment guidelines to be relevant in clinical practice so that novel pharmaceuticals against the specific biomarker targets will be developed.[57,58]

Cancer manifestation is a complex process as it involves many steps including genetic modifications, associated proteins, and signaling pathways. Annexins represent a group of ca^{2+}-related membrane-binding proteins involved in the inflammatory process repair. They play a crucial role in the glucocorticoid-mediated downregulation of the early phase of the inflammatory response. They are also involved in the structural organization of the cell via rearrangement of the

https://doi.org/10.1021/acs.jproteome.3c00484
J. Proteome Res. 2023, 22, 3811−3832

actin cytoskeleton and in intracellular signaling by cell polarization and cell migration.[59]

Calcium/calmodulin (CaM)-dependent protein kinase-II, CaMK (2A, 2B, and 2D) is a multimeric Ser/Thr protein kinase derived from the most predominant proteins in the brain. It is a member of the *N*-methyl-D-aspartate receptor (NMDAR) signaling complex in excitatory synapses that regulate the NMDAR-dependent potentiation of the AMPA receptor and, therefore, excitatory synaptic transmission.[60] It autonomously acts after ca^{2+}/calmodulin-binding and autophosphorylation, and it is involved in synaptic plasticity, neurotransmitter release, and long-term potentiation. It regulates the migration of developing neurons and phosphorylates the transcription factor FOXO3 to activate its transcriptional activity.[60,61]

Proteomic-based approaches have been increased over recent years in cancer-related fundamental science research due to recent advances in mass spectrometry (MS) high-throughput technology with powerful research algorithms, which have facilitated the detection and characterization of potential biomarkers related to exposure or toxic response with high sensitivity and accuracy.[46,58]

The use of 3D in vitro growth of immortalized established cell lines or primary cell cultures is regarded as a more stringent and representative model used to perform viability and cytotoxicity studies that could fill the gap between animal models and conventional 2D monolayer cell cultures since these latter are incapable of reproducing the complexity and heterogeneity of clinical tumors growing with a specific organization and architecture.[62,63]

Overall, the current study was designed and related to the "protein adductomics" concept which is a component of multiomic studies. It is derived from the "exposome" concept that has emerged as a new science to reflect environmental exposures throughout the human lifespan, by considering both external (e.g., exogenous environmental agents) and internal (e.g., endogenous cellular processes) components.[64,65]

In this topic, we have focused on the potential application of an adductomic approach for the screening of xenobiotic adducts on two proteins, ANXA1 and CaMK, as key targets endowed with pivotal roles in human brain tumor pathogenesis. We have first developed a 3D in vitro neurospheroid model derived from human brain tumors and then assessed the potential cytotoxicity effects of IMD and λ-CYH in a binary mixture following 24 h of exposure at IC_{50}. Further, we adopted a bottom-up proteomic-based approach with nano-flow ultrahigh-performance liquid chromatography coupled with tandem mass spectrometry (UHPLC-MS/MS) in order to identify and analyze protein adducts with predicted alteration sites that involved molecular mechanisms. Figure 1 describes the full workflow adaptive methodology for protein adductomics.

2. MATERIALS AND METHODS

2.1. Chemicals and Materials

Imidacloprid (IMD), $C_9H_{10}ClN_5O_2$, *N*-(6-chloropyridin-3-ylmethyl)-2-nitro-imino-imidazo-lidine (CAS number 138261-41-3), and Lambda-cyhalothrin (λ-CYH), $C_{22}H_{19}Cl_2NO_3$ (CAS number 91465-08-6) were selectively purchased as standard solutions of highest purity (≥98%) from Merck KGaA (Germany) and Sigma-Aldrich Chemie GmbH. The molecular structures of these molecules are shown in Figure 1.

Stock solutions of pesticide mixtures were prepared by diluting 150 mg/mL of IMD and 50 mg/mL of λ-CYH in ultrapure water containing 0.01% DMSO (dimethyl sulfoxide) (D8418, Sigma). Then, freshly serially diluted solutions were prepared prior to cytotoxicity analysis.

Ultrapure water was prepared by a Millipore purification system (Billerica, MA, USA).

Dulbecco's phosphate buffered saline (PBS) (D8537), Dulbecco's modified Eagle's medium−high glucose (DMEM) (D5796), Ham's nutrient mixture F12 (51651C), L-glutamine (G7513), trypsin−EDTA (T4049), fetal bovine serum (FBS) (F2442), 1% nonessential amino acid solution (NEAA) (100X) (M7145), neuronal viability serum-free medium supplements N2 (100X) (17502048, GIBCO) and B27 (SCM013), recombinant human epidermal growth factor (EGF) (SRP3027), recombinant human basic fibroblast growth factor (bFGF) (GF003AF), and 1% (v/v) penicillin/streptomycin (P4333) were supplied from Sigma-Aldrich.

Single-cell ultralow attachment 60 mm primaria tissue culture plates (353802) and 25 cm^2 culture flasks (430639) were from Corning Life Science (NY, USA). Corning Costar TC-treated 24-well microplates (CLS3526) were purchased from Sigma-Aldrich.

DL-dithiothreitol (DTT) (3483-12-3), iodoacetamide (IAA) (144-48-9), formic acid (FA) (64-18-6), ammonium bicarbonate (1066-33-7), acetonitrile (ACN) (75-05-8), and methanol (67-56-1) were from Sigma (St. Louis, MO, USA). Trypsin (V5280) taken from the porcine pancreas was purchased from Promega (Madison, WI, USA).

2.2. Ethical Consideration

The procedure carried out in this work was in accordance with the Declaration of Helsinki. It was approved under CPP SUD-0443/2022 by our Ethics Committee attached to the Habib Bourguiba university hospital where this study was conducted. Khemakhem et al. confirmed that our study is in accordance with the code of ethics adopted by the World Medical Association since it is only applied to patients (vulnerable groups) and cannot be carried out in a nonvulnerable group.

The selected participants gave their consent to participate in this research. Written informed consent was obtained from each patient before they underwent any neurosurgery for the possible risks of paralysis or mortality. Additional informed consent was obtained from all individual participants for whom identifying information is included in this article.

2.3. Sample Collection and Culture Conditions

Gliomas and meningiomas (MNGs) represent the most common types of human brain tumors. Medulloblastoma (MDB) is a rare cerebellar embryonal neoplasm that occurs almost exclusively in children.

Our first preliminary experiments were conducted on diverse MNG histological subtypes to check the neurotoxicity of our selected molecules and identify the appropriate inhibitory concentrations (IC_{50}) of pesticides in a binary mixture. In the same way, glioblastoma (GBM) and MDB neurospheroids were developed to assess pesticide neurotoxicity using MS analysis.

Cells were grown in triplicate experiments as neurospheres were derived from six surgical specimens by adopting both enzymatic and nonenzymatic dissociation protocols, as described in the "Supporting Information" file.

https://doi.org/10.1021/acs.jproteome.3c00484
J. Proteome Res. 2023, 22, 3811−3832

To further determine the self-renewal ability to form secondary subspheres, primary spheres were gently dissociated into single cells, plated into a single-cell ultralow attachment plate, and maintained in the neural stem cell culture medium.

We manually inspected neurosphere growth under an inverted phase Contrast microscope (MOTIC AE21, Motic Incorporation Ltd. Hong Kong, China), equipped with an Axiocam camera 208 [Sony CMOS image sensor color, rolling shutter; square pixels of 1.85 μM side length; 3840 × 2160 pixel resolution; ultra HD (4K); 3 × 8 bits/pixel] (Zeiss, France) at scale bars of 100 μm, 150, and 200 μm before proceeding.

2.4. IHC Staining

Primary cell identity was confirmed prior to use by immunohistochemical (IHC) staining for neuronal differentiation markers such as NSE (neuron-specific enolase) (IMGENEX, Cat# IMG-80398, RRID:AB_1151008), chromogranin (Fitzgerald Industries International Cat# 10R-C126ax, RRID:AB_1283819), synaptophysin (IMGENEX Cat# IMG-80349, RRID:AB_1151989), GFAP (glial fibrillary acidic protein) (IMGENEX, Cat# IMG-80134, RRID:AB_1150393), and Ki67 proliferation marker (Bio-Rad Cat# MCA289, RRID:AB_321740).

We also analyzed "stemness" gene expressions, including CD133 (BD Biosciences Cat# 747569, RRID:AB_2744141), CD44 (BD Biosciences Cat# 558739, RRID:AB_397098), CD24 (BD Biosciences Cat# 555426, RRID:AB_395820), Nestin (IMGENEX Cat# IMG-6492A, RRID:AB_2033866), SOX1 (BD Biosciences Cat# 562224, RRID:AB_11154034), SOX2 (BD Biosciences Cat# 560291, RRID:AB_1645334), and βIII-tubulin (Promega Cat# G7121, RRID:AB_430874).

Both primary cells and multiple 3D spheroids were harvested and processed into histological blocks that, after standard fixation and embedding procedures, were sectioned to produce slides for IHC staining; the detailed protocol is described in the "Supporting Information" file.

2.5. Chemical Treatment

We have adopted the protocol described by Roper and Coyle at the University of Nottingham, studying the effects of drug cytotoxicity on in vitro 3D spheroid models.[66] We visually inspected plates under bright-field microscopy to assess the growth and health of neurospheres.

Images were imported and analyzed using Image-Pro Plus analyzer software, V7.0 (Media Cybernetics, Inc., Bethesda, MD, USA) (www.adept.net.au/software/mediacy/ImagePro/imageProPlus.shtml, RRID: SCR_007369).

After 7 days, when primary cultured cells reached the optimal size of 250−350 μm in diameter, we measured the coefficient of variation (CV) to confirm uniformity in spheroid volume or size reproducibility prior to treatment.

Five serial diluted concentrations of pesticide binary mixtures had been used ranging from 2.95 μM (754 ng/g) to 0.59 mM (151 × 10^3 ng/g) of IMD and 0.55 μM (247 ng/g) to 0.11 mM (49.5 ng/g) of λ-CYH, based on our preliminary investigations conducted on MNGs to measure appropriate cytotoxic inhibitory concentrations in human brain tumor neurospheroids since cells are generally less sensitive in 3D compounds compared to 2D compounds.

We gently removed 100 μL of neurosphere medium from each plate and added 100 μL of pesticide mixture and then incubated it for 24 h in a humidified incubator at 5% CO_2/37 °C. Three replicates per concentration were analyzed. Untreated control cells were also used in each analysis by changing 100 μL of media with 100 μL of 0.01% DMSO. At the end of the exposure period, toxicity end points were determined in both control and exposed neurospheroids.

2.6. Monitoring Spheroid Viability

Cell viability was performed by both the MTT assay and microscopy to assess morphological changes and the histopathological profiles of tumor tissues.

2.6.1. MTT Assay Viability. After 24 h of pesticide treatment, neurospheroids seeded into 24-well microplates were treated with 0.5 mg/mL MTT for 4 h. Following incubation, dark blue formazan crystals were solubilized with 1:1 (v/v) DMSO/isopropanol. Each well was resuspended until the dissolution of crystals. Then, the optical density was measured at 570 nm by using a Spectramax plate reader (Multiskan Spectrum, Thermo Electron Corporation). The percent viability was expressed as the ratio of the absorbance in the experimental wells to that of the control wells (set as 100%). A dose−response curve was generated and the IC_{50} value (concentration required for 50% growth inhibition) of IMD and λ-CYH in a binary mixture was calculated using nonlinear regression analysis.

2.6.2. Assessing Morphological Changes. The morphological changes in the shape and density of the spheroids after pesticide exposure were evaluated by microscopy.

2.6.3. Histopathological Profile Analysis. Hematoxylin and eosin (H&E) represents the combination of two histological stains, namely, hematoxylin and eosin. Pieces of tissues were collected, frozen at −20 °C, cut on a cryostat rotary manual, a microtome that cuts frozen tissue (MICROM HM 505 N), fixed, and stained with H&E, followed by rinsing with water, 95° alcohol, and xylene before being fixed by special glue stick preservation. The H&E-stained sections were examined for histopathological analysis. This method was also applied to assess cytotoxic responses based on tumor neurospheroid proliferation following pesticide treatment.

2.7. Sample Preparation and Protein Extraction

After 24 h of pesticide treatment, our samples consisted of three treated vs nontreated brain tumor spheroids; these were harvested, pooled in a centrifuge tube, washed with cold PBS at 4 °C, centrifuged at 2500*g* for 10 min, and then collected and lyophilized by a freeze-dryer (CHRIST). Proteins were extracted by the modified RIPA lysis buffer (50 mM Tris-HCl, pH 7.4, 150 mM NaCl, 1% Triton X-100, 5 mM EDTA, pH 8.0) containing 1× protease inhibitor cocktail (HALT, Thermo scientific) and phosphatase inhibitor cocktail (1 mM NaVO4, 50 nM NaF) (Thermo Scientific), then assayed by the BCA kit after which 100 μg of proteins were reduced by 50 mM ammonium bicarbonate and 10 mM DTT at 56 °C for 1 h and alkylated by 20 mM IAA in the dark for 1 h, and then digested at 37 °C overnight by a free trypsin at a ratio of 1:50. The extracted peptides were lyophilized and then resuspended in 20 μL of 0.1% formic acid before analysis by MS.

2.8. Analysis by Nanoflow UHPLC-ESI-MS/MS

Samples were analyzed using a high-resolution mass spectrometry that consisted of an Ultimate 3000 nano UPLC system (Thermo Fisher Scientific, USA) with a Q Exactive HF hybrid quadrupole-Orbitrap mass spectrometer (Thermo Fisher Scientific, USA), an ESI nanospray source, and a higher energy collisional dissociation (HCD) fragmentation mode. The nanocolumn comprises a trapping column (PepMap C18,

https://doi.org/10.1021/acs.jproteome.3c00484
J. Proteome Res. 2023, 22, 3811−3832

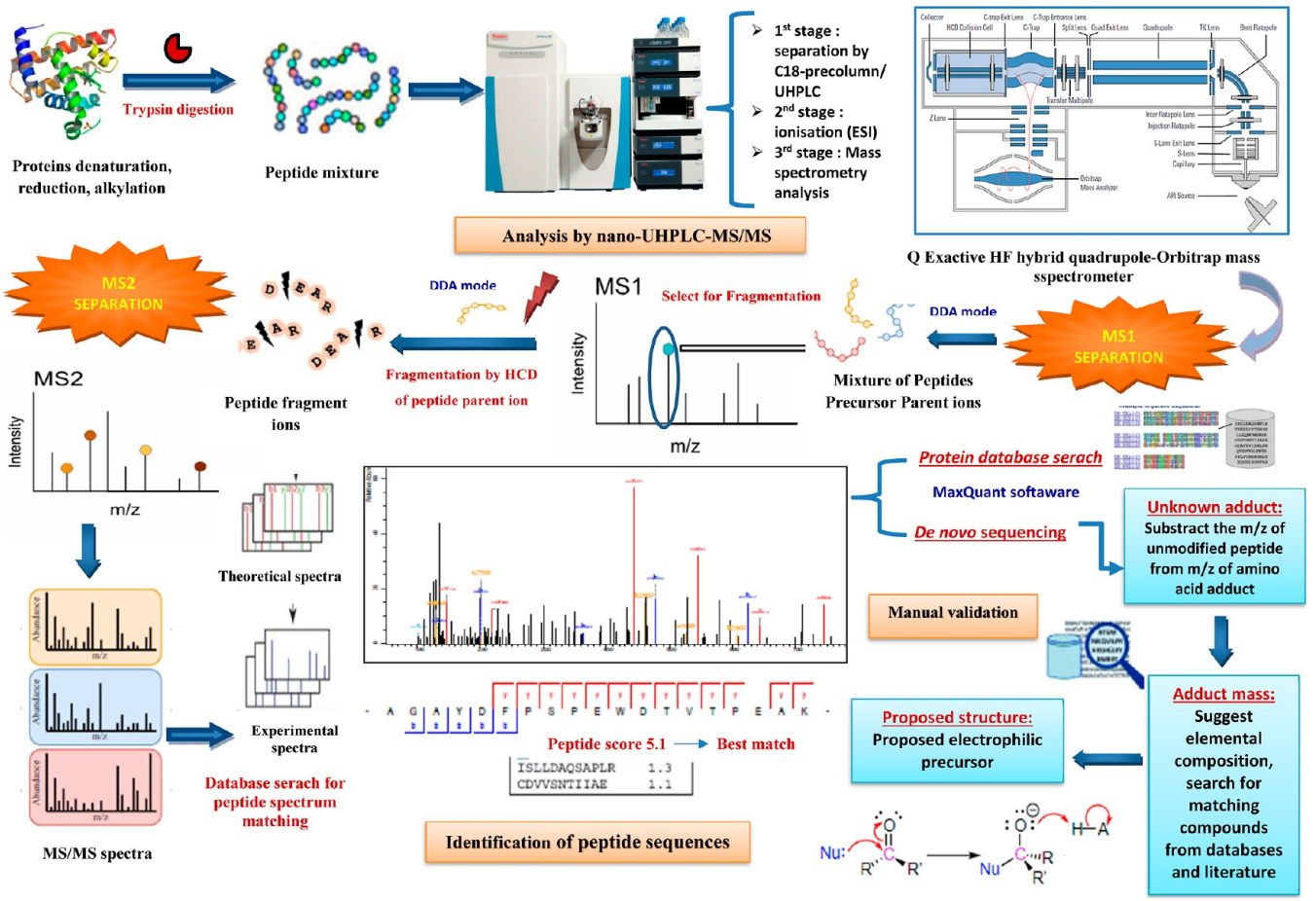

Figure 2. Workflow depicting the process of a typical untargeted bottom-up proteomic approach-based MS analysis for the screening and characterization of protein adducts: (1) dissociate tissues; lyse cells, denature proteins with, e.g., urea/detergents; (2) reduce disulfides with, e.g., DTT; alkylate cysteines with, e.g., IAA; (3) purify proteins by precipitation; (4) digest proteins with a protease; (5) resuspend peptides in a LC−MS compatible solvent, e.g., 0.1% formic acid in water; (6) clean with, e.g., a C18 precolumn and run with UHPLC-MS/MS; (7) process raw data by a suitable software package (MaxQuant); (8) perform database search for peptide spectrum matching and protein identification; (9) FDR control and *de novo* sequencing: compare MS/MS spectra between treated and nontreated samples for manual interpretation; (10) Subtract m/z of unmodified peptide from the m/z of the amino acid adduct; suggest elemental composition; (11) search for matching compounds (databases and literature) and propose the structure. (2) DTT: DL-dithiothreitol; IAA: iodoacetamide; DDA: data-dependent acquisition mode; HCD: higher energy collisional dissociation; MS1/MS2: tandem mass spectrometry; FDR: false discovery rate.

100 Å, 100 μm × 2 cm, 5 μm) and an analytical column (PepMap C18, 100 Å, 75 μm × 50 cm, 2 μm). The loading amount was 1 μg, and the total flow rate was 250 nL/min. The mobile phase consisted of solvent A (0.1% formic acid in water) and solvent B (0.1% formic acid in 80% acetonitrile) by linear gradient: from 2 to 8% buffer B in 3 min, from 8 to 20% buffer B in 56 min, from 20 to 40% buffer B in 37 min, and then from 40 to 90% buffer B in 4 min.

The full scan was performed between 300 and 1650 m/z at a resolution of 60 000 at 200 m/z. The automatic gain control target for the full scan was set at 3×10^6. The MS/MS scan was operated in the top 20 mode using the following settings: resolution 15 000 at 200 m/z; automatic gain control target 1×10^5; maximum injection time 19 ms; normalized collision energy at 28%; isolation window of 1.4 Th; charge state exclusion: unassigned, 1, >6; dynamic exclusion 30 s.

2.9. Data-MS Analysis and Protein Identification

Raw MS files were analyzed and searched against a human protein database based on the species of the samples using the MaxQuant (V.1.6.1.14, RRID: SCR_014485) search engine. The parameters were set as follows: protein modifications were carbamidomethylation (C) (fixed) and methionine oxidation (variable); the enzyme specificity was set to trypsin with two maximum missed cleavages; the precursor ion mass tolerance was 10 ppm; and the MS/MS fragment ion tolerance was 0.6 Da.

Proteins were identified with a high confidence interval at 95%, containing at least one identified peptide. The proteome profiles between the two groups were compared using a false discovery rate (FDR) ≤ 0.05 as the threshold to judge the significance in protein expression maps' difference. Only proteins identified three times were considered. Proteins were filtered into two categories, namely, "upregulated" with positive values and "downregulated" with negative values, based on the log 2 FC criteria and using the paired t-test with a P value threshold of 0.05.

Scaffold (version 4.10.0, Proteome software, Inc., Portland, OR) was used to validate the MS/MS based peptide and protein identification.

https://doi.org/10.1021/acs.jproteome.3c00484
J. Proteome Res. 2023, 22, 3811−3832

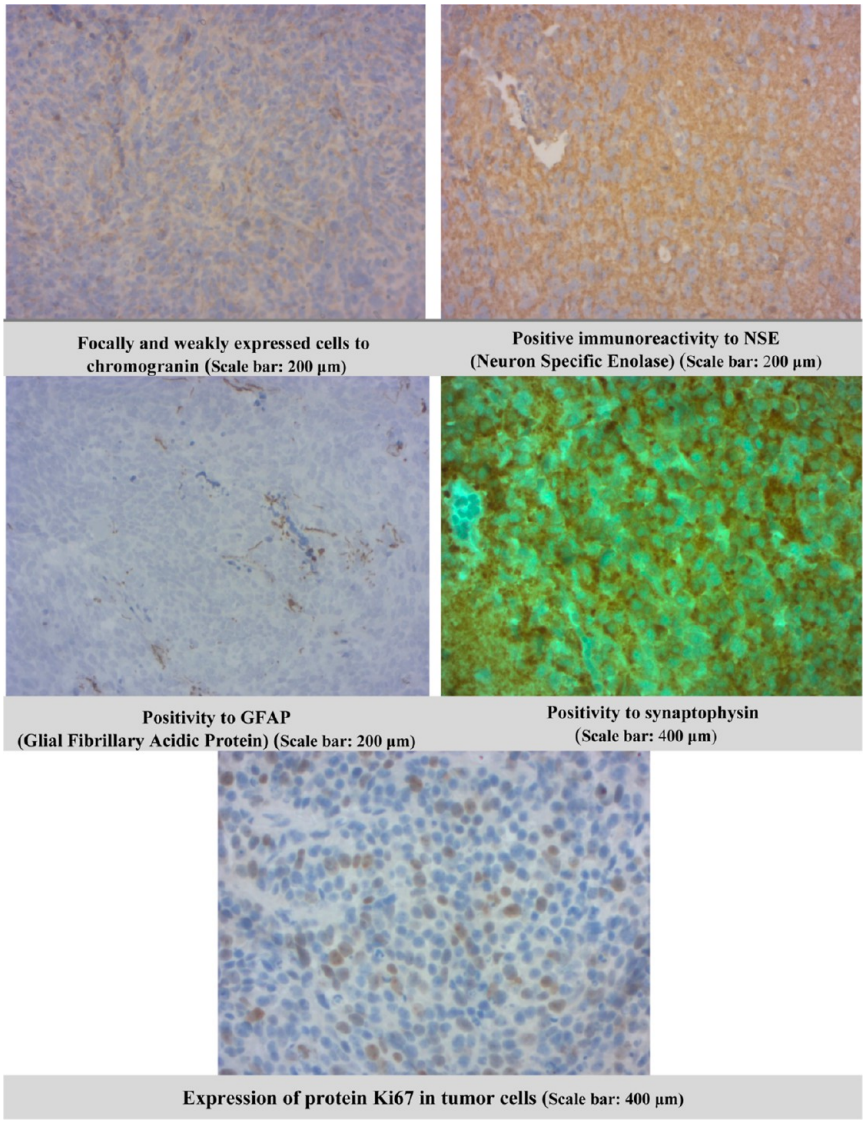

Figure 3. Immunohistochemical analysis for neuronal differentiation markers: (A) focally and weakly expressed cells to chromogranin (scale bar: 200 μm); (B) positive immunoreactivity to NSE (scale bar: 200 μm); (C) positivity to GFAP (scale bar: 200 μm); (D) positivity to synaptophysin (scale bar: 400 μm); and (E) expression of protein Ki67 in tumor cells (scale bar: 400 μm).

2.10. Screening of Protein Adduct Formation by *De Novo* Sequencing

To study proteins' adduct formation, we adopted an untargeted proteomic-based approach using high-resolution tandem mass spectrometry. On this platform, the ionization was performed in a positive-ion mode, and the mass spectrometer was operated in the data-dependent acquisition (DDA) mode, which selects the most abundant ions that give the strongest signals in the first x tandem mass spectrometry stage (MS1) to be fragmented and analyzed in the second tandem mass spectrometry stage (MS2).

Proteins adducts were identified using *de novo* sequencing, which consisted of comparing the MS/MS spectra of peptide sequences between treated and nontreated spheroids. The precursor parent ion of the tryptic peptide fragment was singled out and analyzed in the second MS spectrum after dissociation into smaller fragments to determine the amino acid sequence of the peptide fragment and subsequently identify the modification sites in the MS2 spectra.

This procedure of manual verification allowed the classification of unknown compounds as adducts as well as the determination of adduct masses by subtracting the m/z of the unmodified amino acid from the m/z of the amino acid adduct. Afterward, the calculated added masses were used to propose the elemental compositions of adducts and to suggest the likely structures and electrophilic precursors. The negative added masses were assigned to truncations and deletions (ion losses).

Adducts' hypotheses about possible annotations were then validated using database searching tools and calculator softwares. The chemistry of the specific nucleophilic sites and the presence of reactive functional groups (e.g., double bonds, aldehyde, and epoxide) in the electrophilic structure to form adducts had been also taken into consideration.

The full workflow schematic illustration of the shotgun proteomic-based adaptive strategy in our case study of protein adductomics is shown in Figure 2.

https://doi.org/10.1021/acs.jproteome.3c00484
J. Proteome Res. 2023, 22, 3811−3832

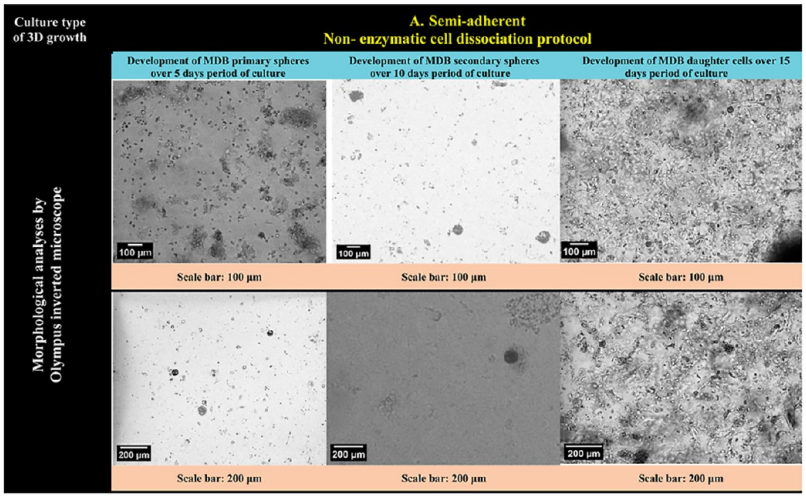

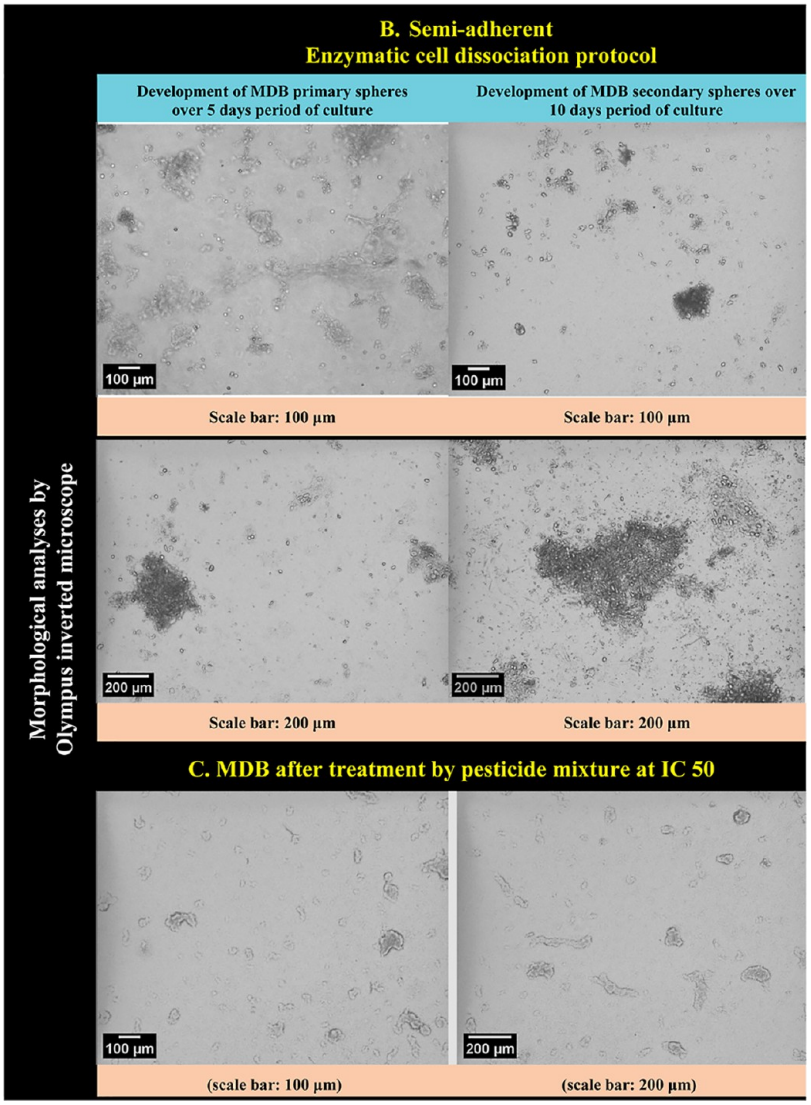

Figure 4. 3D neurospheroid culture model developed from human MDB stem-like cells before pesticide treatment. Representative images of 3D spheroids' growth captured by an inverted-phase Contrast microscope (MOTIC AE21, Motic Incorporation Ltd., Hong Kong, China) equipped with an Axiocam camera 208 [Sony CMOS image sensor color, rolling shutter; square pixels of 1.85 μM side length; 3840 × 2160 pixel resolution; ultra HD (4K); 3 × 8 bits/pixel] (Zeiss, France). Selected images were performed with a magnification of 100 and 200 μm. (A) For semiadherent culture type, adapting the nonenzymatic cell dissociation protocol, MDB stem-like cells could proliferate and form within 5 days multipotent floating cell clusters called primary spheres (left panels) that have self-renewal features and continuously form secondary subspheres after another five added days of culture (middle panels). Both primary and secondary spheres could form daughter MDB adherent cells on day 15:

https://doi.org/10.1021/acs.jproteome.3c00484
J. Proteome Res. 2023, 22, 3811−3832

Figure 4. continued

morphologically, neurites begin to extend; the cells displayed spindle-form or polygonal to amorphous shapes and grow as adherent forms of cells on culture dishes. (B) Enzymatic cell dissociation protocol: cultured tumor cells could more swiftly generate primary and secondary spheres but with less developed and robust morphology than those isolated straight from the fresh tumor. (C) Microscopy analysis of MDB neurospheroids' viability and morphology after treatment by pesticide mixture (imidacloprid + λ-cyhalothrin) at IC_{50} [30.33 μM (7754.2 ng/g) of IMD and 5.75 μM (2584.7 ng/g) of λ-CYH]: a high number of cells with large vacuoles and small round- and nonuniform-shaped cells (typical of cells being detached from the plate). Cell density was greatly reduced, mainly presenting cellular debris.

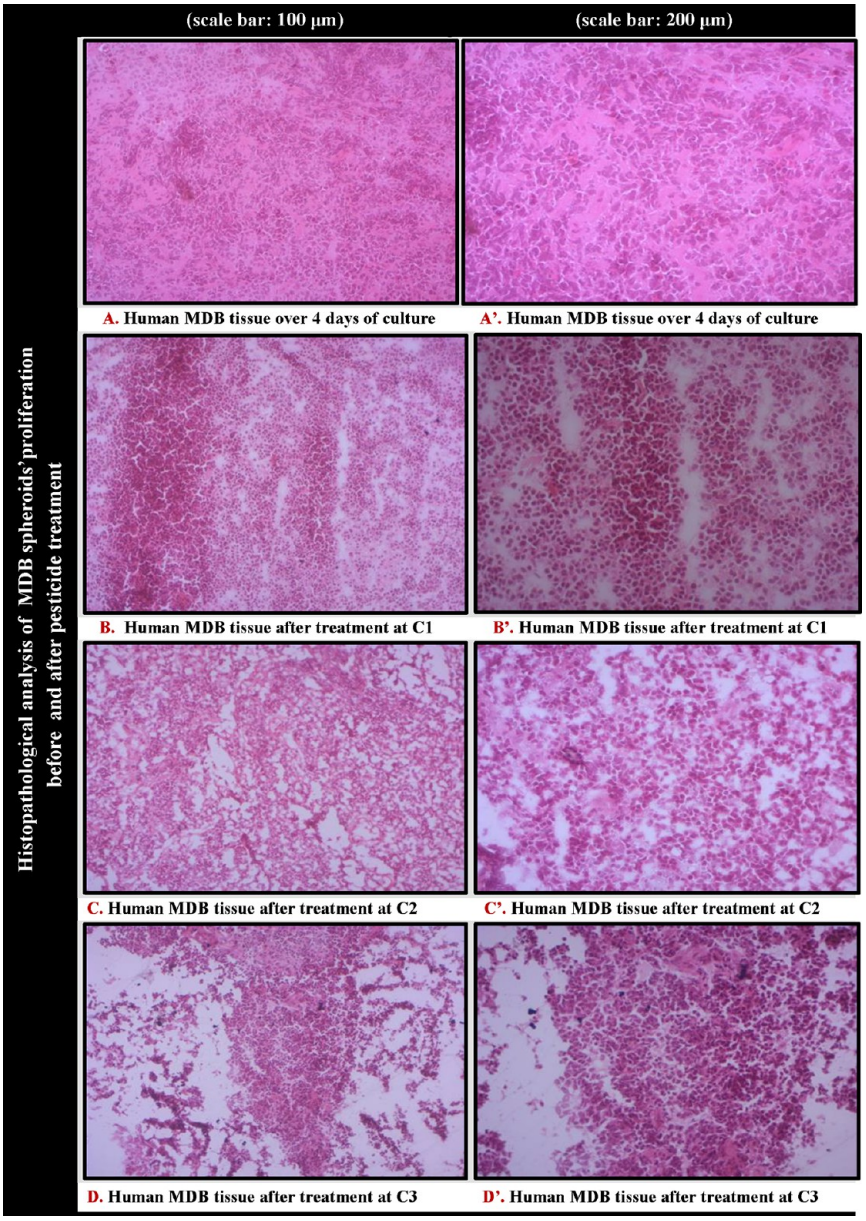

Figure 5. Representative microphotographs of histopathology shown on H&E staining obtained from frozen sections of MDB spheroids before and after 24 h of pesticide treatment (magnification ×100 and 200). (A) (H&E×100) and A′ (H&E×200): MDB with high cell density proliferation over 4 days of culture. (B) (H&E×100) and B′ (H&E×200): moderate cell density proliferation after low dose of pesticide treatment at C1:2.95 μM (754 ng/g) of IMD + 0.55 μM (247 ng/g) of λ-CYH. (C) (H&E×100) and C′ (H&E×200): weak cell density proliferation with light appearance of apoptotic and necrotic cells after a moderate dose of pesticide treatment at C2:5.9 μM (1508 ng/g) of IMD + 1.1 μM (494.8 ng/g) of λ-CYH. (D) (H&E×100) and D′ (H&E×200): very weak cell density proliferation with diffuse appearance of apoptotic and necrotic cells after high dose of pesticide treatment at C3:0.59 mM (150.8×10^3 ng/g) of IMD + 0.11 mM (49.5×10^3 ng/g) of λ-CYH.

2.11. Other Statistical Analysis

Data performed by GraphPad Prism software (Version.8, San Diego, CA, USA) are expressed as mean values with ±standard deviation (SD), and the statistical significance of differences between counts was determined using the unpaired Student's *t*-test. P values ≤ 0.05 were statistically significant. For each separate experiment, three replicates were carried out.

https://doi.org/10.1021/acs.jproteome.3c00484
J. Proteome Res. 2023, 22, 3811−3832

3. RESULTS

3.1. IHC Staining of MDB Brain Tumors

IHS for neuronal differentiation markers had shown positive immunoreactivity to NSE and focal and weak cell expression to chromogranin, synaptophysin, and GFAP. The expression of protein Ki67, which is strongly associated with cellular proliferation and widely used as a marker of the mitotic index in tumors, was evaluated at 2% and increased to 30% in anaplastic areas (Figure 3).

3.2. Isolation of MDB Tumor Stem-Like Cells and Characterization of Sphere Formation and Stemness Markers

For the semiadherent culture type, the nonenzymatic protocol was adopted, and the dissociated cells derived from freshly human surgical specimens were grown as colonies. After 3 days of incubation, primary homogeneous tumor cells appeared in a fusiform format and were arranged in multidirectional cultural bundles. Then, growth factors were added to the medium. Two days later, these primary cells gave rise to primary sphere formation (Figure 4A, left panels).

Moreover, to check their self-renewal capacity, these primary spheres were gently dissociated to single cells and maintained in a stem cell culture medium in which after 5 days, we observed secondary subsphere formation (Figure 4A, middle panels), confirming that MDB stem-like cells are capable of self-renewal. After five more days of culture, both primary and secondary spheres could form daughter adherent cells (Figure 4A, right panels). In the same way, spheroids were generated more swiftly using an enzymatic cell dissociation protocol, leading to the development of a heterogeneous population of cell proliferation in 10 days. Based on these two protocols, we highly appreciated that the primary tumor sphere culture could generate neurospheres with more developed and robust morphology compared with those isolated straight from the fresh tumor (Figure 4B). Thus, our further experiments were only carried out on a 3D spheroid model isolated from nonenzymatically dissociated cells.

Growth and morphological changes of neurospheres were monitored for several days, regarding changes in shape and size evolution. On day seven, spheroids reached diameters of 250−350 μm. The CV was inferior to 20%, proving the reproducibility in the spheroid size over three different experiments.

Concerning an in-depth analysis of stemness features, neurospheroids were analyzed by using IHC staining. In particular, we considered (i) the expression of CD133, Nestin, SOX1, and SOX2 as indicative of stemness markers; (ii) GFAP and CD44 as astrocytic markers; (iii) CD24 and βIII-tubulin as representative of neuronal progenitors or highly neuronal differentiated cells, respectively. Results indicated positive stemness gene expressions for Nestin, CD44, GFAP, βIII-tubulin, and Ki67 but lack them for CD133+, SOX1, SOX2, and CD24.

3.3. Assessment of Cell Viability and Proliferation Following Pesticide Treatment

Besides MTT assay, cell viability and proliferation were also monitored after 24 h of pesticide exposure by counting the number of survival spheres. The surviving fraction represents the number of neurospheres normalized to controls. Student's *t*-test was applied to indicate statistical significance ($P < 0.05$) (Figure S1). Based on our previous experiments on MNG, the IC_{50} value (required for 50% growth inhibition) of the pesticide mixture calculated from the dose−response curve using nonlinear regression analysis was 30.33 μM (7754.2 ng/g) of IMD and 5.75 μM (2584.7 ng/g) of λ-CYH, respectively. These concentrations were also suitable to assess cytotoxicity responses to MDB after 24 h in the range of [IC_{30}-IC_{60}] confirmed by histopathological analysis.

Photomicrographs of H&E-stained sections of cultured MDB neurospheroids before and after treatment, illustrated in Figure 5, were analyzed to assess their viability and proliferation. The results showed that the viability was decreased by increasing concentrations. This proves that pesticides used in the mixture may interact to mitigate cell density proliferation with the appearance of apoptotic and necrotic cells. Microscopy analysis also confirmed significant morphological changes brought about by pesticide treatment, evidenced by the presence of large vacuoles and small round- and nonuniform-shaped cells, with significant loss in density and an increase in cellular debris (Figure 4C).

3.4. Identification and Characterization of Pesticide −Adduct-Induced Alteration in CaMK2 and ANXA1 Proteins by Using *De Novo* Sequencing

The comparative analysis of dynamic proteomic profiles between treated and nontreated spheroids revealed that both ANXA1 and CaMK2 proteins were expressed at down-regulation, which confirms their alterations induced by pesticide treatment. Table 1 summarizes the expression profiles of the selected proteins.

De novo sequencing revealed several alterations in the active site of 82-ANXA1 by adduct formation (Figure 6, available on PDF in the original format in the data repository) in comparing the spectra of treated and nontreated spheroids. The predicted added mass shifts were, namely, (+128.09 Da) assigned as 1,3-dimethyl-3,4,5,6-tetrahydro-2(1*H*)-pyrimidinon ($C_6H_{12}N_2O$), respectively, on the C-terminal of 97-Lys (lysine), 96-Leu (leucine), 85-Leu, 89-Gly (glycine), 88-Thr (threonine), and 86-Gln (glutamine) residues; (+128.59 Da) on the C-terminal of 95-Thr residue; (127.59 Da) on the C-terminal of 92-Leu residue; (+13.06 Da) on 93-Asp (aspartic acid) residue; (31.04 Da) assigned as methyl-amine (CH_3NH_2) on the C-terminal of 91-Pro (proline) residue; (74.55 Da) on the C-terminal of 94-Glu (acid glutamic) residue; (291.15 Da) assigned as tripelennamine hydrochloride ($C_{16}H_{22}ClN_3$) on the C-terminal of 84-Tyr (tyrosine); and (+362.19 Da) on the C-terminal of 83-Ala (alanine) residue.

On the N-terminal of 85-Leu and 86-Gln residues, the added mass shift of either (+113.08 Da) or (+241.1 Da) could be predicted as 2-chloropyridine (C_5H_4ClN) and 1,3-dimethyl-5-nitroimidazolium perchlorate ($C_5H_8ClN_3O_6$) adduct formation, respectively.

In the active site of 228-CaMK2 presented in Figure 7 (available on PDF in the original format in the data repository), we also identified, by using peptide sequencing, adduct formation that was envisaged by the added mass shifts (+129.04 Da), (+87.03 Da), and (+147.07 Da) on the C-terminal of 237-Glu, 235-Ser (serine), and 233-Phe (phenylalanine) residues, respectively, which could be predicted as difluoroaniline ($C_6H_5F_2N$), propene-2-nitro ($C_3H_5NO_2$), and 2-methoxyphenyl-acetonitrile (C_9H_9NO). The masses of b ions were identical.

All of these modifications were detected in a triplicate analysis. Peptide sequences and the predicted fragment ions

https://doi.org/10.1021/acs.jproteome.3c00484
J. Proteome Res. 2023, 22, 3811−3832

Table 1. Protein Expression Profile of ANXA1 and CaMK2[a]

MaxQuant[a] accession no.	protein ID[b]	gene names	MW[c] (kDa)	peptide matched[d]	sequence coverage[e] (%)	Log 2 fold change ($P < 0.05$)	function
P04083	annexin A1	ANXA1	38.714	18 (18)	57.2	−1.65	calcium/phospholipid binding/calcium signaling/inflammatory process
A5A6M2							
P07150							
Q9UQM7	calcium/calmodulin-dependent protein kinase type II subunit alpha; calcium/calmodulin-dependent protein kinase type II subunit delta; calcium/calmodulin-dependent protein kinase type II subunit gamma; calcium/calmodulin-dependent protein kinase type II subunit beta	CAMK2A	54.087	2 (2)	36.5	−0.52	calcium signaling at glutamatergic synapses
Q13557		CAMK2D					
Q13555		CAMK2G					
Q13554		CAMK2B					

[a]Accession numbers from the MaxQuant database. [b]Protein ID from the MaxQuant database. [c]Theoretical molecular weight (MW). [d]Number of matched peptides versus total number of peptides. [e]Coverage of the matched peptides in relation to the full-length sequence.

are illustrated next to each tandem mass spectrum. Ion losses such as dehydration and deamination induced by HCD fragmentation are also mentioned.

Table 2 reports the calculated added mass shifts with the predicted elemental composition and the possible adduct structures or their corresponding electrophilic precursors.

4. DISCUSSION

4.1. Isolation of Tumor Stem-Like Cells from Human Brain Medullobalstoma and Characterization of Sphere Formation

Tumor stem-like cells can be defined as tumor-initiating cells in a wide spectrum of malignant tumors.[67−75] Cultured human brain tumor cells could proliferate and generate multipotent floating cell clusters called neurospheres.[75,76] In a spheroid model, cell aggregates in suspension generated 3D conformations that are not attached to an external surface of support. These cells provided more biologically relevant data than 2D monolayers due to the natural cell-to-cell interactions, hypoxia, drug penetration, response to resistance, and the production of an extracellular matrix.[74,77]

The aim of this study was achieved by applying the following approaches: (i) collecting; (ii) establishing of primary cell cultures; (iii) isolating neurospheres derived from these primary cultures (primary neurospheres); and (iv) developing secondary neurospheres or subspheres.

Prior to 3D spheroid generation, cells were grown under their standard 2D culture conditions. A serum-free neurosphere medium, containing supplements and growth factors, was added to the maintenance of tumor stem-like cells with properties similar to those of the primary tumor avoiding spontaneous cell differentiation.[66,78]

After a 7 day culture period, spheres reached a size range of 250−350 μm in diameter. This size range represents the optimal size for permitting drug perfusion and establishing pathophysiological oxygen gradients throughout the spheroid.[77,79] A diameter greater than 500 μm was unsuitable since it was characterized by hypoxic regions and necrotic centers.[79] Before proceeding with cytotoxicity tests, since several morphological parameters, such as spheroid volume and shape, affect responses, and given that the number of exposed cells may respond differently to the chemicals being a source of variability, and due to the necessity of a preselection of tumor spheroids of homogeneous volume and shape to reduce data variability to a minimum, we have proved the reproducibility in spheroid size by calculating the CV of spheroid volumes on day 7 based on image analysis using Image-Pro Analyzer software, which was described as a perfectly acceptable alternative technique applied to cytometers.[77] Our 3D spheroids are therefore considered a valid model.

Characteristic features of tumor stem-like cells include spherical formation, self-renewal to secondary neurospheres or subspheres, and stem-like markers of their corresponding parental tumors.[80] In our study, the developed MDB neurospheroids displayed enhanced self-renewal with the expression of stemness and neuronal differentiation markers.

4.2. Effects of Pesticide Mixture on Neurospheroid Proliferation and Viability

Histological staining performed before and after pesticide treatment (Figure 5) allowed target validation by visualizing tumor spheroid area proliferation and viability. This protocol was suitable for the assessment of cytotoxic responses.

https://doi.org/10.1021/acs.jproteome.3c00484
J. Proteome Res. 2023, 22, 3811−3832

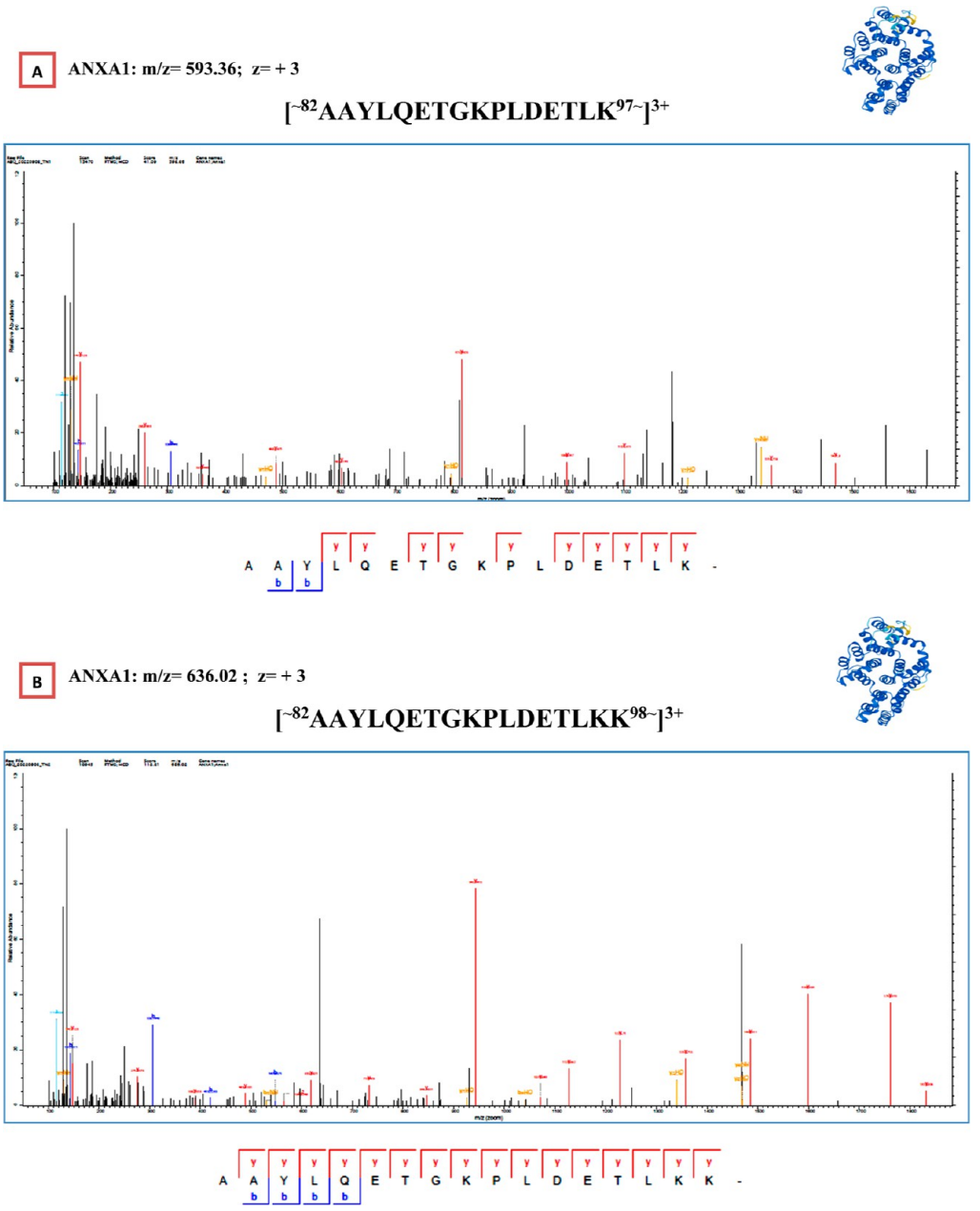

Figure 6. MS/MS spectra of the peptide sequence containing the active site of ANXA1 obtained after isolation and fragmentation of the tryptic peptide precursor ion, respectively, for nontreated (A) and treated (B) spheroids. (A) $[^{\sim 82}$AAYLQETGKPLDETLK$^{97\sim}]^{3+}$ with MW (molecular weight) 1775.93 Da, $[M + 3H]^{3+}$ ion at the monoisotopic mass of 592.98 Th (average m/z = 593.36). (B) $[^{\sim 82}$AAYLQETGKPLDETLKK$^{98\sim}]^{3+}$ with MW 1904.03 Da, $[M + 3H]^{3+}$ ion at the monoisotopic mass of 635.68 Th (average m/z = 636.02). The MS/MS spectra are available on PDF original format in the data repository. Monoisotopic mass refers to the sum of atomic masses using the most abundant naturally occurring isotope for each atom. Da: daltons; Th: Thomson. The 3D-structure of ANXA1 gene was from the Human Gene Database (Gene Card).

Our study revealed that pesticides used in the mixture may interact to inhibit the proliferation of tumor tissue and weaken neural cell density with the progressive appearance of apoptotic and necrotic cells. These results were confirmed by previous studies showing that pyrethroids may additionally contribute in a notable way to the deleterious effects of pesticide mixtures.[81]

Indeed, Alvim and Martinez (2019) have identified a synergistic interaction between IMD and λ-CYH in both blood and the liver to induce DNA damage, high protein carbonylation, and lipid peroxidation and found that the result of such interaction had led to an increased toxicity in shorter time, proving that the effects of pesticides in mixture are mainly due to the presence of a pyrethroid.[82] In addition, significant synergistic responses were also revealed by these pesticides used in ternary and quaternary mixtures.[83]

The neurotoxicity effect was observed at concentrations much higher than the reported average daily intake estimated at 57 μg/kg body weight (bw)/day for IMD[84] and 2.5 μg/kg bw/day for λ-CYH.[85] Based on the repeated dose toxicity studies summarized by JMPR (Joint FAO/WHO Meeting on Pesticide Residues; 2002), NOAEL (no observed effect level) of 52.5 μg/kg bw/day applying the default uncertainty factor of 100 and NOAL of 0.5 mg/kg bw/day applying the default uncertainty factor of 200 were, respectively, established for the

https://doi.org/10.1021/acs.jproteome.3c00484
J. Proteome Res. 2023, 22, 3811−3832

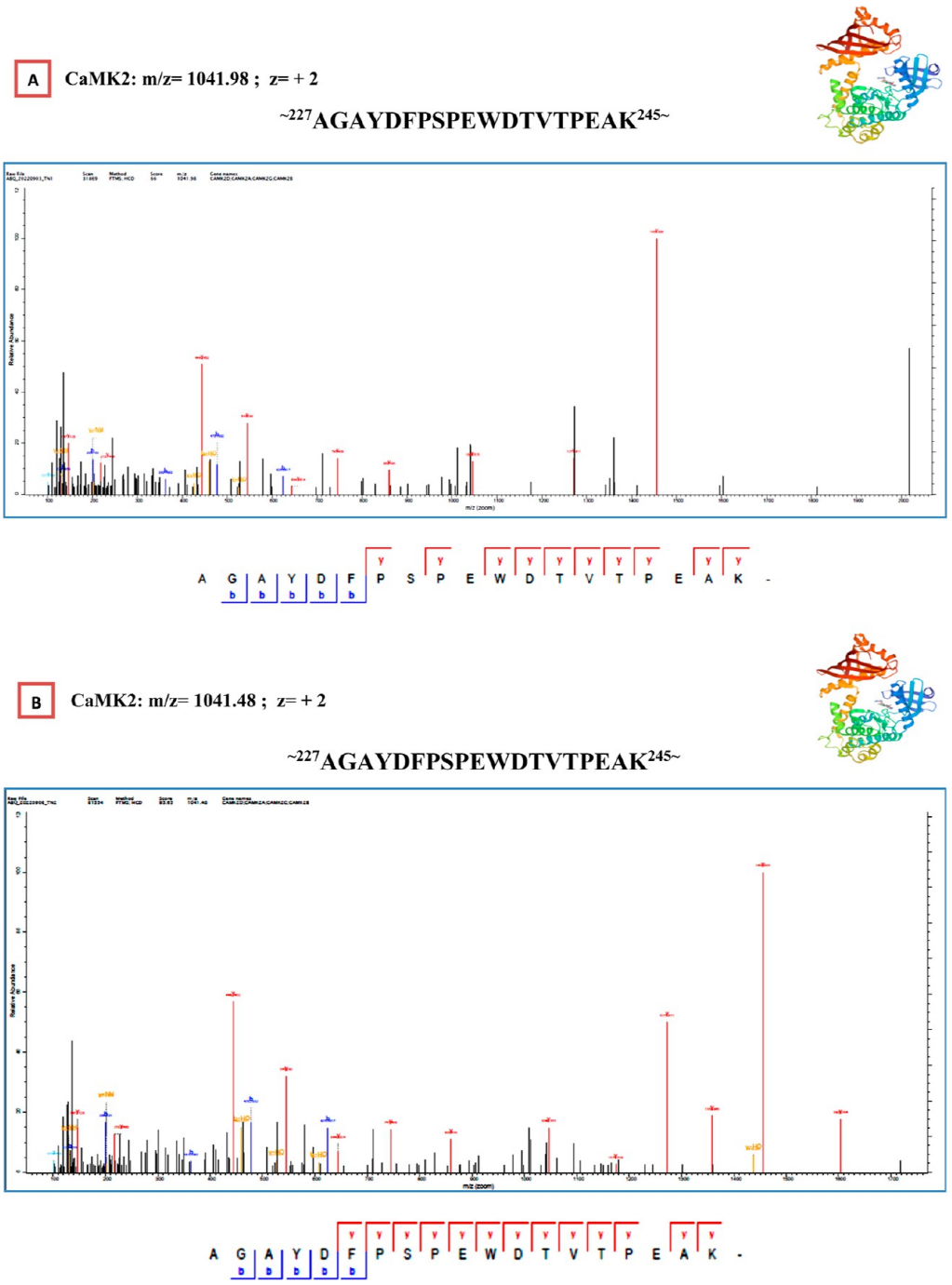

Figure 7. MS/MS spectra of the peptide sequence containing the active site of CaMK2, [~227AGAYDFPSPEWDTVTPEAK245~]2+ obtained after isolation and fragmentation of the tryptic peptide precursor ion of MW 2079.84 Da, $[M+2H]^{2+}$ ion at the monoisotopic mass of 1040.97855 Th, and average m/z = 1041.98 and 1041.48, respectively, for nontreated (A) and treated (B) spheroids. The MS/MS spectra are available on PDF original format in the data repository. Monoisotopic mass refers to the sum of atomic masses using the most abundant naturally occurring isotope for each atom. Da: daltons; Th: Thomson. The 3D-structure of CaMK2A gene (as an example from CaMK2 family) was from the Human Gene Database (Gene Card).

assessment risk of IMD[86] and λ-CYH on the basis of neurotoxicity signs.[87]

Overall, these high cytotoxic concentrations make it unlikely that any neurological alterations in environmental regulatory human exposure.

4.3. Identification and Characterization of Adduct Formation on CaMKII and ANXA1 Proteins by Using De Novo Sequencing

For the study of proteins' adduct formation, we advocated a more pragmatic "fit-for-purpose" approach, which balances methodological rigor with cost. Thus, we have adopted an untargeted proteomic-based approach using a high-resolution tandem mass spectrometry which has been the analytical detection technique of choice for adduct measurement due to

https://doi.org/10.1021/acs.jproteome.3c00484
J. Proteome Res. 2023, 22, 3811−3832

Table 2. Protein Adductomics: The Suggested Adduct Formation on CaMKII and ANXA1 Proteins by Peptide Sequencing

proteins	observed m/z ions for nontreated spheroids	observed m/z ions for treated spheroids	added mass shift (Da)	suggested elemental composition of added mass shift by the NIST[a] database	annotation
the active site of 82-ANXA1	1471.8	1599.895	+128.09	1,3-dimethyl-3,4,5,6-tetrahydro-2(1*H*)-pyrimidinon ($C_6H_{12}N_2O$)	C-terminal of
	1358.716	1486.811			85-Leu
	1101.615	1229.71			86-Gln
	1000.567	1128.662			88-Thr
	260.1969	388.2918			89-Gly
	147.1128	275.2078			96-Leu
					97-Lys
	361.2445	489.8395	+128.59	unknown	C-terminalof 95-thr residue
	605.8141	733.409	+127.59	unknown	C-terminal of 9 2-Leu residue
	605.8141	618.8821	+13.07	unknown	C-terminal of 93-Asp
	815.4509	846.4931	+31.04	methyl-amine (CH_3NH_2)	C-terminal of 91-Pro
	490.2871	564.8348	+74.55	unknown	C-terminal of 94-Glu
	1471.8	1762.959	+291.15	tripelennamine hydrochloride ($C_{16}H_{22}ClN_3$)	C-terminal of 84-Tyr
	1471.8	1833.996	+362.19	unknown	C-terminal of 83-Ala
	306.1448	419.2289	+113.08	2-chloropyridine (C_5H_4ClN)	N-terminal of 85-Leu
	306.1448	547.2875	+241.14	1,3-dimethyl-5-nitroimidazolium perchlorate ($C_5H_8ClN_3O_6$)	N-terminal of 86-Gln
the active site of 228-CaMK2	1046.515	1175.558	+129.04	difluoroaniline ($C_6H_5F_2N$)	C-terminal of 237-Glu
	1272.611	1359.643	+87.03	propene-2-nitro ($C_3H_5NO_2$)	C-terminal of 235-Ser
	1456.695	1603.764	+147.07	2-methoxyphenyl-acetonitrile (C_9H_9NO)	C-terminal of 233-Phe

[a]NIST: National Institute of Standards and Technology.

its high sensitivity and accuracy in providing both qualitative and quantitative information, which have facilitated the identification of thousands of modified proteins and xenobiotic adduct formation in a single experiment.

Following this untargeted detection of adducts, the most challenging is to identify the mechanistically important ones due to the potential vastness in their structural diversity and the lack of a common "handle" by which we can purify and identify adducts. Indeed, compared with both metabolomics and proteomics, there is neither commercial software nor a specific database to evaluate adductomic data. The only information available to formulate hypotheses on adduct identities are a list of adducts detected, with their molecular weights, estimated concentrations (by quantitative method), and retention times.[64,88] This procedure of manual identification or "*de novo* sequencing" is more time-consuming when compared to automated approaches that apply recently developed software packages, such as PepNovo+, PAEKS, and especially UniNovo, which is reported to be the best in facilitating the manual validation of Orbitrap MS data.[89]

The widespread use of these recent bioinformatic search engines with powerful algorithms for protein search databases, as well as the development of more robust workflows using targeted or semitargeted scanning routines and the improvement of enrichment strategies and chemical labels have simplified and accelerated proteomics analysis. However, in view of MS potential pitfalls, the manual interpretation is rather straightforward and still needed data validation to avoid false-positive data and obtain precise information on the identity and the location of the modified amino acid within the peptide, e.g., the identification of incorrectly assigned oxidation to proline by *de novo* sequencing when using a probability-based search engine, reviewed by Verrastro et al.[90] Therefore, we proceeded in our study with a manual identification of protein adducts.

The accuracy of the calculated added mass relies on the type of mass spectrometer and the database search engine performance, which is our case study not only in adopting the Q-Exactive hybrid quadrupole-Orbitrap tandem mass spectrometry that provides more accurate data but also in using MaxQuant software, as a famous platform for LC−MS/MS shotgun proteomics that achieves peptide mass accuracies with high sequencing coverage, thanks to its advanced nonlinear recalibration algorithms.[91]

From an analytical standpoint, after elemental compositions for unknown adducts are proposed, the validation of identities can be assisted by other methods, such as database searching, calculator software, and the comparison of measured and predicted physicochemical properties. However, at some stages, a synthetic reference compound would be needed to confirm a particular adduct's identity and to implicate the corresponding electrophile.[64]

In our case study, to facilitate the hypothesis on possible annotations, we have opted for some tools, namely, the UNIMOD database that lists protein modifications (www.unimod.org),[92] the Molecular Formula finder, provided by ChemCalc (http://www.chemcalc.org/mf_finder),[93] and the "Search for Species Data by Molecular Weight" given by the

https://doi.org/10.1021/acs.jproteome.3c00484
J. Proteome Res. 2023, 22, 3811−3832

National Institute of Standards and Technologies (NIST) (https://webbook.nist.gov/chemistry/mw-ser),[94] which lists species based on their input values.

Thus, using a likely composition, adduct structure, or the corresponding precursor electrophiles has been suggested. Concerning low-mass adducts, there are only a few possible structures that facilitate the adduct identification process. However, for molecular weights (MWs) of >70 Da, there are many possibilities that make such annotations difficult.

Moreover, to validate the identities of mechanistically important adducts since they can be formed by the neurotoxicant in multiple nucleophilic residues on proteins, we have searched the MEDLINE and ISI Web of Science databases by using some key terms, namely, "adductomics", "adducts of calmodulin", "adducts of Annexin", and "adducts detection in cell lines", alone and in combination with other keywords, such as "detection", "intoxication", "exposure", "adverse effects", and "toxicity." In addition, we have screened for additional relevant studies including nonindexed reports in applicable Internet resources.

As regards the predicted physicochemical properties, protein adducts are usually covalent modifications formed via a nucleophilic substitution in which reactive drugs are metabolized in vivo to an electrophilic form by endogenous (e.g., oxidative stress) or exogenous (e.g., diet) sources. These reactive species which commonly have reactive functional groups can attack nucleophilic atoms (especially O, N, and S) at the side chains of amino acid residues, notably the sulfhydryl group of cysteine and amine functionalities of histidine, lysine, and N-terminal amino acids. Thus, adducts could be formed either via nucleophilic substitution (the case of oxygen radicals and epoxides) or via Michael addition (the case of α, β-unsaturated carbonyl compounds) or as Schiff bases via carbinolamine intermediates (the case of aldehydes). The extent of adduct formation is included not only by the nucleophilicity and pK_a of the nucleophile atom to have free electron pairs but also by the steric factors influencing the access of reactive electrophilic sites to form covalent bonds.[88]

In summary, untargeted proteomic-based approaches remain promising tools for protein adductomics. They tend to complement the targeted methods rather than replacing them. Indeed, approaches that combine both methods have been proposed.[90,95]

4.4. Elucidation of the Neurotoxicity Mechanism Induced by Pesticide Treatment

Several environmental pollutants can cause programmed cell death or apoptosis in animals and humans.[96,97] Brain tissue is particularly vulnerable to oxidative damage due to its relatively low antioxidant capacity, high consumption of oxygen, glucose, and energy, large amounts of fatty acids, and high content of easily oxidized substrates (preferred ROS targets).[11]

Xenobiotic toxicity is highly dependent on some defined physicochemical characteristics which predict its potential interaction with cell membranes and its ability to permeate them. Based on the literature review, our selected molecules exhibit low molecular weight and high liposolubility that can easily be absorbed across all biological membranes, including mitochondrial and hematoencephalic barriers.[98] These characteristics provide insights into their potential cytotoxicity to target brain tissues.

Proteins, as one of the major targets for oxygen free radicals and other reactive species, could be altered either via a direct attack by free radicals (metal-catalyzed oxidation), or via backbone oxidative cleavage, or via lipid peroxidation end-products, such as isoketals, malondialdehyde, and 4-hydroxy-2-trans-nonena, or via the reaction of reducing sugars or their oxidation products.[99] Although cells have developed antioxidant defense that protects them from free radicals,[100] some of them escape defense attacks and modify subcellular components.[101]

Pesticides which cannot bind covalently to macromolecules share as a possible mechanism of toxicity the ability to trigger apoptosis through alterations in redox homeostasis generated by oxidative stress following the net production of ROS, especially in mitochondria, which can result in the onset of cell dysfunction as an impairment of antioxidant enzyme function. Furthermore, oxidative stress can be detrimental to several interacting mechanisms including direct damage to crucial molecular species, an increase in intracellular free Ca^{2+}, and a release of excitatory amino acids.[11,102]

By way of illustration, we report here the molecular targets of the selected pesticide molecules.

Pyrethroids have the ability to bind and impair mammalian voltage-gated channels, including sodium, calcium, and potassium ions, which block their closure, leading to a permanent depolarization of axonal membranes and paralysis defining the insecticidal action.[103,104] Pyrethroids can also impair γ-aminobutyric acid (GABA) and glutamate receptors as well as hormone receptors[105,106] and affect drug transporters which are key actors in the drug detoxification system such as ATP-binding cassettes and solute carrier transporters which include multidrug resistance-associated proteins (MRP)2, breast cancer resistance proteins, organic anion transporter polypeptides, multidrug and toxin extrusion transporters, and organic cation transporters reported to be inhibited by allethrin and tetramethrin.[81]

Pyrethroids were reported to affect DNA through peroxidase action leading to the production of semiquinones and quinones, which are capable of forming DNA adducts.[107] In addition, quinolones potentially affect the DNA topoisomerase II, an enzyme that participates in DNA repair and recombination, which may induce double-strand breaks modifying the DNA topology.[107] They were also reported to induce nitric oxide (NO) that reacts with the superoxide radical to form highly reactive peroxynitrite (ONOO−). The latter provokes cellular damage by interacting with guanine, leading to nitrative and oxidative DNA lesions, such as 8-NO_2-Gua and 8-oxo-deoxyguanosine (8-OHdG), respectively.[107] Interestingly, λ-cyh was demonstrated to interact with enzymes belonging to the purinergic system involved in the metabolism of extracellular nucleotides and nucleosides.[108]

IMD, like other neonicotinoids, shares a structural similarity and a common mode of action with the tobacco toxin nicotine. Its toxicity was attributed to the alteration of neurotransmission in the nicotinic cholinergic nervous system in that due to its hydrophobic character, it binds to the nicotinic acetylcholine receptors at both neuronal and neuromuscular junctions, resulting in prolonged stimulation, desensitization, receptor blocking, and, thus, cell death.[109]

The identification of proteins affected by xenobiotic adduct formation and the elucidation of the involved molecular mechanism help to diagnose novel biomarkers and pave the way for new therapeutic strategies to target neurotoxicity with minimum side effects.

https://doi.org/10.1021/acs.jproteome.3c00484
J. Proteome Res. 2023, 22, 3811−3832

Several toxicological research studies have focused on diverse protein arrays. In our case study, to look for regulator and effector proteins in cancer pathogenesis, ANXA1 and CaMKII have been selected as key target proteins since both are endowed with pivotal roles, implicated in calcium homeostasis, and expressed in tumor progression and invasion.

Annexin-1 (ANXA1), a calcium-dependent phospholipid-binding protein, is an old widely reported protein investigated in a variety of different fields including cardiology, neurology, endocrinology, and oncology. In fact, ANXA1 has long been classified as an anti-inflammatory protein due to its control over leukocyte-mediated immune responses. However, it is now recognized to have multiple pathophysiological roles and widespread effects beyond the immune system with implications in maintaining the homeostatic balance within the entire body due to its ability to affect cellular signaling, hormonal secretion, fetal development, the aging process, and disease development.[110] However, its role to date is yet to be fully unveiled.

Deregulated expression of ANXA1 has been involved in tumorigenesis. They were associated with the development and progression of a large number of cancers, namely, lung cancer,[111,112] colorectal cancer,[113−115] hepatocellular carcinoma,[116] melanomas,[117] pancreatic cancers,[118] and brain cancers.[119,120] High levels of ANXA1 promoted tumor invasion and metastasis to be positively correlated with disease severity and poor survival.[60] Contrariwise, some cancers were developed at downregulated ANXA1 expressions, such as prostate cancer,[121−123] esophageal carcinomas,[123−126] lymphoma,[127] larynx cancer,[128] and nasopharyngeal carcinoma.[129]

ANXA1 is also endowed with a key role in the brain as it is expressed in many neurovascular unit cells, including brain endothelial cells, microglial cells, astrocytes, pericytes, and neurons, where it provides neuroprotective and repair functions.[110] In our previously published study conducted on IDH mutant high grade gliomas,[119] we have identified the annexin A protein family (ANXA1, ANXA2, ANXA4, ANXA5, ANXA6, and ANXA7) altered by pesticide treatment and expressed in tumor progression and metastasis as calcium-regulatory proteins. Other recent studies have also involved the role of ANXA1 in the development and progression of malignant gliomas,[60,120] especially GBM, by increasing the IL-8 expression through NF-κB (p65) activation, leading to the immune escape in GBM.[120]

Hence, ANXA1 was assigned to act as an important biomarker of diagnosis and prognosis for a variety of cancer types. It was effectively selected as a FDA-approved therapeutic target.[60]

CaMK2 also plays a vital role in promoting cancer progression, including growth, proliferation, invasion, and metastasis.[130−132] In our recent publication dealing with IDH mutant high-grade gliomas,[119] we have emphasized the potential role of CaMK2 that could be assigned as a prognostic indicator of high-grade astrocytomas involved in tumor invasion and metastasis. Indeed, He, Q. and Li, Z (2021) have reported the role of CaMK2γ as a potential candidate for predicting GBM prognosis in which the altered transcript level was more closely associated with the tumorigenesis and recurrence of high-grade gliomas, compared to low-grade astrocytomas.[132] CaMK2 was also involved in regulating the stemness of the GBM cells. The altered activity of CaMK2γ abolished not only stem-like traits, such as cell growth and neurosphere formation, but also the protein levels of GSC stemness markers, such as CD133, Nanog, Sox2, and Oct4.[132] Moreover, CaMK2γ was reported in the therapeutic resistance found at overexpressions to enhance the chemoresistance of liver cancer cells to 5-fluorouracil and that of ovarian cancer cells to cisplatin.[132]

There are plenty of contradictory studies in the literature for the role of CaMK2, found to be both pro-apoptotic[133,134] and anti-apoptotic.[131] On the one hand, it was revealed that the increased Ca^{2+} level resulting from reticulum endoplasmic stress induced the expression of the FAS death receptor through a pathway involving (CaMK2γ) and JNK (c-Jun N-terminal kinase). It was also shown that CaMK2γ induced mitochondrial-dependent apoptosis by releasing cytochrome *c* and losing mitochondrial membrane potential. On the other hand, CaMK2 is involved in cancer development, cell migration, invasiveness, and metastasis development.[131]

Although the role of CaMK2 in cancer remains ambiguous, as reported in different contradictory studies, there is most evidence by informatics analysis for its critical role in cancer development, metastasis, resistance, recurrence, and the sustentation of GBM-cell stemness markers. Thus, CaMK2 may also be a novel promising approach for a therapy of IDH mutant high-grade gliomas, e.g., calmodulin inhibitors were reported to trigger the proteolytic processing of membrane type 1 metalloproteinase to a bound-inactive form and to enhance the tissue inhibitors of MMP expression levels, resulting in a loss of migratory potential of U87MG cells.[135]

Overall, both selected proteins were proven to be affected by stressors and to play critical roles in a variety of malignant diseases. Consequently, they could be assigned for potential therapeutic targets whose modulation presents new opportunities for diagnosis and treatment strategies,[60,136] e.g., mediating the neurotoxicity effect through binding of specific target nucleophiles in these key neuronal proteins.

Although protein adductomics is a challenging concept, it remains a powerful bioanalytical tool for the verification of xenobiotic exposure with high sensitivity and well-understood toxicity mechanisms, facilitated by recent advances in proteomic methodologies and MS high-throughput techniques.

Based on the literature review, previous studies have not yet applied the use of proteomics-based approaches for screening xenobiotic adducts that induce alteration in ANXA1 and CaMKII proteins. Only a few reports on dysregulated CaMKII activities induced by PTMs have been described. The CaMKII activity upon stimulation by Ca^{2+}/CaM is regulated by phosphorylation on two highly conserved phosphosite sets in the regulatory segment (Thr 286 and Thr 305/Thr 306). CaMKII activation results in downstream phosphorylation and several targets at the synapse.[61] It was demonstrated that CaMKII mutations at the highly conserved Thr residues in the regulatory segment result in learning and memory impairments.[61] In addition to phosphorylation, other PTMs such as methionine oxidation and serine glycosylation have been reported at sites near the critical stimulatory phosphosite. Covalent modification of 279-Ser by O-linked *N*-acetylglucosamine was reported under hyperglycemic conditions of diabetes mellitus as key contributors of cardiopathological conditions associated with diabetes.[137]

Thus, to the best of our knowledge, we report here for the first time the mechanistic molecular interactions of two pesticides to induce neurotoxicity effects in a 3D human brain tumor neurospheroid model. On the basis of pesticide chemical structures, we have summarized their most relevant

https://doi.org/10.1021/acs.jproteome.3c00484
J. Proteome Res. 2023, 22, 3811−3832

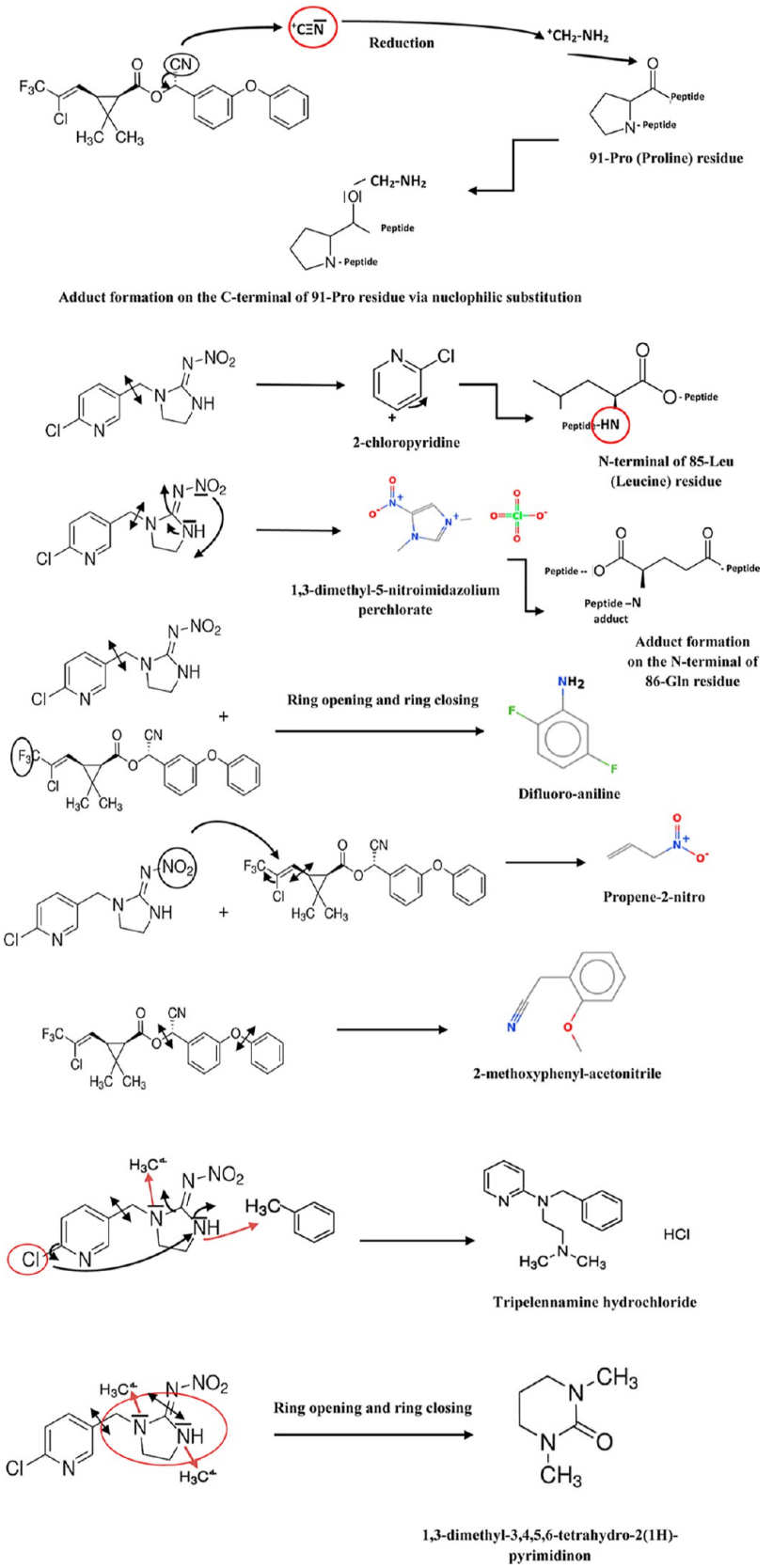

Figure 8. Summary of the most mechanistically important molecular interactions between pesticide molecules (λ-cyhalothrin and imidacloprid) to yield the predicted protein adducts formed via a covalent bond that governs reactions between xenobiotic electrophiles and nucleophilic sites on the C-terminal or N-terminal of amino acid residues in both 82-ANXA1 and 228-CaMK2 active sites.

mechanistic molecular interactions (Figure 8) to yield the predicted adducts formed via nucleophilic substitution on the C-terminal or N-terminal of amino acid residues in both active 82-ANXA1 and 228-CaMK2 sites, as described previously.

https://doi.org/10.1021/acs.jproteome.3c00484
J. Proteome Res. 2023, 22, 3811−3832

These modifications play a crucial role in the toxicity mechanism since they impair protein active sites and/or molecular structures and consequently impair their biological roles, especially for those endowed with a pivotal function such as our CaMK2 and ANXA1 case. The results of such alterations can have toxicological impacts such as neurotoxicity since a protein with adduct formation accumulates and reaches a sufficient level for pathway failure, which ultimately causes damage to submembrane organelles, metabolic pathways, or cytological processes, leading to nerve injury and cell apoptosis. Hence, the decreased level of CaMK2 could be involved in the apoptegenic pathway signaling.

Overall, the neurotoxicity effect observed in our selected pesticide molecules used in the mixture may be due to either the added cytotoxicity effect of each molecule target or their molecular interactions yielding protein adduct formation since many neurotoxicants are electrophiles. Our study gives a bird's eye view that pyrethroids may additionally contribute in a notable way to deleterious effects of pesticides used in mixture.

5. CONCLUSIONS

Protein damage or DNA modification by the reactive intermediates of chemical carcinogens is a key early event in the carcinogenic process as well as other chronic diseases.

Although many previous studies in the literature have focused on the toxic effects of pesticides on human health risk assessment processes, relatively little is known about the potential interactions that may occur between pesticides in mixture. For the majority, the corresponding molecular mechanisms of neurotoxicity are poorly understood.

Toxicoproteomics, integrating proteomic knowledge into toxicology, is gaining much research interest facilitated by recent advances in MS instruments and bioinformatic tools, which have allowed high-throughput analysis for the simultaneous identification of thousands of modified peptides with insights into alteration sites and characterization of xenobiotic adducts, including their biological roles as well as their application as putative biomarkers for toxicity diagnosis.

To the best of our knowledge, our study is the first investigation that applied a 3D neurospheroid model with a shotgun proteomic-based approach for assessing pesticide mixture-induced neurotoxicity and elucidating the involved molecular mechanism. Our findings gave the first evidence that the neurotoxicity effect of IMD and λ-CYH used in a binary mixture was related to their molecular interactions to yield protein adducts by covalently binding small molecules. These modifications play a crucial role in the toxicity mechanism since they alter protein structures and therefore impair their biological functions, especially for those endowed with a pivotal role. Thus, neurotoxicity could be mediated through the binding of specific target nucleophiles in key neuronal proteins.

Although, the identification of protein adducts remains a complicated and time-consuming procedure, combining automated and manual interpretations/validations generally leads to the best reliable information. The recent development of specific databases, such as the Toxic Exposome Database (T3DB) (http://www.t3db.ca)[138] and the Exposome-Explorer Database (http://exposome-explorer.iarc.fr)[139] could also be a relevant way for the evaluation of adductomic data. Moreover, tremendous progress in the MS technology will facilitate adductomics and address key bottlenecks in the identification of protein modifications by decreasing detection limits and improving mass accuracies.

Finally, despite some studies having yet to emerge, it is anticipated that new insights into the importance of environmental factors in the etiology of human diseases will ensue, aiding us to monitor human exposures to hazardous health effects to help take necessary preventive measures in order to avoid the occurrences of such diseases.

6. APPENDICES

$$V(\mu m^2) = \frac{4}{3} \times \pi r^3 \quad \text{(A)}$$

$$\text{CV in \%} = \frac{\text{standard deviation of spheroid diameter}}{\text{mean spheroid diameter}} \times 100 \quad \text{(B)}$$

V: volume, r: radius, CV: coefficient of variation

■ ASSOCIATED CONTENT

Data Availability Statement

The data that support the findings of this study are openly available. Data that support the finding of this study, including peptide sequencing and protein identification, are available at the ProteomeXchange Consortium via the MassIVE partner repository (for shotgun proteomics data) at: https://massive.ucsd.edu/ProteoSAFe/QueryPXD?id=PXD043000 With the data set identifier:Username: MSV000092168_reviewerPassword: REVIEWER100.

Supporting Information

The Supporting Information is available free of charge at https://pubs.acs.org/doi/10.1021/acs.jproteome.3c00484.

Additional experimental methods of 3D neurospheroid culture protocols, additional experimental method of immunohistochemical staining, and spheroid survival following pesticide exposure (PDF)

■ AUTHOR INFORMATION

Corresponding Author

Kaouthar Louati − *Faculty of Pharmacy, Laboratory of Pharmacology, Analytics & Galenic Drug Development-LR12ES09, University of Monastir, Monastir 5000, Tunisia;* orcid.org/0000-0001-5085-4766; Phone: +216 92 761 162; Email: kaoutharlouati66@gmail.com, kaouthar.louati@fphm.u-monastir.tn

Authors

Amina Maalej − *Laboratory of Environmental Bioprocesses, Centre of Biotechnology of Sfax, Sfax 3018, Tunisia*

Fatma Kolsi − *Department of Neurosurgery, Habib Bourguiba University Hospital, Sfax 3089, Tunisia; Faculty of Medicine, Avenue of Majida Boulila, University of sfax, Sfax 3029, Tunisia*

Rim Kallel − *Laboratory of Pathological Anatomy and Cytology, Habib Bourguiba University Hospital, Sfax 3089, Tunisia; Faculty of Medicine, Avenue of Majida Boulila, University of sfax, Sfax 3029, Tunisia*

Yassine Gdoura − *Department of Neurosurgery, Habib Bourguiba University Hospital, Sfax 3089, Tunisia; Faculty of Medicine, Avenue of Majida Boulila, University of sfax, Sfax 3029, Tunisia*

https://doi.org/10.1021/acs.jproteome.3c00484
J. Proteome Res. 2023, 22, 3811−3832

Mahdi Borni − *Department of Neurosurgery, Habib Bourguiba University Hospital, Sfax 3089, Tunisia; Faculty of Medicine, Avenue of Majida Boulila, University of sfax, Sfax 3029, Tunisia*
Leila Sellami Hakim − *Laboratory of Pathological Anatomy and Cytology, Habib Bourguiba University Hospital, Sfax 3089, Tunisia*
Rania Zribi − *Higher Institute of Applied Studies to Humanities of Tunis (ISEAHT), University of Tunis, Tunis 1005, Tunisia*
Sirine Choura − *Laboratory of Environmental Bioprocesses, Centre of Biotechnology of Sfax, Sfax 3018, Tunisia*
Sami Sayadi − *Biotechnology Program, Center for Sustainable Development, College of Arts and Sciences, Qatar University, Doha 2713, Qatar*
Mohamed Chamkha − *Laboratory of Environmental Bioprocesses, Centre of Biotechnology of Sfax, Sfax 3018, Tunisia*
Basma Mnif − *Department of Bacteriology, Habib Bourguiba University Hospital, Sfax 3089, Tunisia; Faculty of Medicine, Avenue of Majida Boulila, University of sfax, Sfax 3029, Tunisia*
Zouheir Khemakhem − *Legal Medicine Department, Habib Bourguiba University Hospital, Sfax 3089, Tunisia; Faculty of Medicine, Avenue of Majida Boulila, University of sfax, Sfax 3029, Tunisia*
Tahya Sellami Boudawara − *Laboratory of Pathological Anatomy and Cytology, Habib Bourguiba University Hospital, Sfax 3089, Tunisia; Faculty of Medicine, Avenue of Majida Boulila, University of sfax, Sfax 3029, Tunisia*
Mohamed Zaher Boudawara − *Department of Neurosurgery, Habib Bourguiba University Hospital, Sfax 3089, Tunisia; Faculty of Medicine, Avenue of Majida Boulila, University of sfax, Sfax 3029, Tunisia*
Fathi Safta − *Faculty of Pharmacy, Laboratory of Pharmacology, Analytics & Galenic Drug Development-LR12ES09, University of Monastir, Monastir 5000, Tunisia*

Complete contact information is available at: https://pubs.acs.org/10.1021/acs.jproteome.3c00484

Author Contributions

K.L. (the corresponding author): conceptualization, investigation, writing—original draft, methodology, formal analysis, data curation, and writing—review & editing; F.K., Y.G., M.B., and B.M.: investigation and resources; R.K., L.S.H., and T.S.B.: validation; A.M. and S.C.: formal analysis and software; R.Z.: writing—review & editing; S.S.: resources; M.C.: resources and project administration; M.Z.B.: supervision; Z.K.: project administration and visualization; and F.S.: supervision. All authors have approved the final paper.

Funding

This research did not receive any specific grant from funding agencies in public, commercial, or non-for-profit sectors.

Notes

The authors declare no competing financial interest.

■ ACKNOWLEDGMENTS

Our study was supported by the Ministry of Higher Eduction and Ministry of Health, Tunisia. Our deepest and most sincere gratitude and thanks go to (1) our representative authorities of the medical ethics committee, (2) the head of the Pathological Anatomy department and the Cytology Laboratory in Habib Bourguiba medium hospital and her team due to their support in histopathological diagnosis, (3) neurosurgeons: all our neurosurgical doctors who have performed successful surgeries by taking into consideration their patients' safety and all teams in the neurosurgery department for their help; (4) Sirine Choura, Amina Maalej, and Mohamed Chamkha for their technical assistance and help by providing the necessary materials for stem-like cells' culture in the Biotechnology center, Sfax, Tunisia; (5) Rania Zribi for proofreading this work by taking into account the English language; (6) the pharmaceutical team of Habib Bourguiba medium hospital for providing necessary surgical materials. I am also immensely grateful to Dr A. Wijesekara, A. Kocon, and Dr W. Carter for their precious help and support while conducting my first experimental analysis in assessing pesticide toxicity in the School of Medicine, Royal Derby Hospital Center, University of Nottingham, UK. My special thanks are extended to Dr Lively J., and Ren S., for performing for us a facility service (Proteomics, USA).

■ ABBREVIATIONS

λ-CYH, lambda-cyhalothrin
3D, three-dimensional
ACN, acetonitrile
Ala, alanine
ANXA1, annexin-A1
Asp, aspartic acid
BFGF, basic human fibroblast growth factor
CaMK2, calcium calmodulin-dependent protein kinase-II
CV, coefficient of variation
DDA, data-dependent acquisition
DMEM, Dulbecco's modified Eagle's medium
DMSO, dimethylsulfoxide
DNA, deoxyribonucleic acid
DTT, DL-dithiothreitol
EDTA, ethylene diamine tetra-acetic acid
EGF, epidermal growth factor
ESI, electrospray ionization
FA, formic acid
FAS, fas cell surface death receptor
FDA, US Food and Drug Administration
FBS, fetal bovine serum
FDR, false discovery rate
FG, fold-change
FOXO3, forkhead box O3
GATA3, trans-acting T-cell-specific transcription factor
GFAP, glial fibrillary acidic protein
GBM, glioblastoma
Gln, glutamine
H&E, hematoxylin and eosin
HCD, higher energy collisional dissociation
IAA, iodoacetamide
IC_{50}, the median inhibition concentration
IDH, isocitrate dehydrogenase
IHC, immunohistochemical
IMD, imidacloprid
JNK, c-Jun N-terminal kinase
Leu, leucine
Lys, lysine
MDB, medulloblastoma
MNG, meningioma
MS, mass spectrometry

https://doi.org/10.1021/acs.jproteome.3c00484
J. Proteome Res. 2023, 22, 3811−3832

MTT, 3-[45-dimethylthiazol-2-yl]-2,5 diphenyl tetrazolium bromide
MW, molecular weights
NEAA, nonessential amino acids
NO, nitric oxide
NOAEL, no observed effect level
NSE, neuron-specific enolase
PBS, phosphate buffered saline
Phe, phenylalanine
Pro, proline
PTMs, protein post-translational modification
ROS, reactive nitrogen species
SD, standard deviation
Ser, serine
SOX1, SRY-box transcription factor 1
Thr, threonine
Tyr, tyrosine
UHPLC, ultrahigh-performance liquid chromatography

REFERENCES

(1) Sharma, A.; Kumar, V.; Shahzad, B.; Tanveer, M.; Sidhu, G. P. S.; Handa, N.; Kohli, S. K.; Yadav, P.; Bali, A. S.; Parihar, R. D.; et al. Worldwide pesticide usage and its impacts on ecosystem. *SN Appl. Sci.* **2019**, *1*, 1446.

(2) Cabras, P.; Angioni, A. Pesticide residues in grapes, wine, and their processing products. *J. Agric. Food Chem.* **2000**, *48*, 967−973.

(3) Zambonin, C. G.; Quinto, M.; De Vietro, N.; Palmisano, F. Solid-phase micro-extraction - gas chromatography mass spectrometry: a fast and simple screening method for the assessment of organophosphorus pesticides resi-dues in wine and fruit juices. *Food Chem.* **2004**, *86*, 269−274.

(4) Burnett, M.; Welford, R. Case study: coca-cola and water in India: episode 2. *Corp Soc. Responsib Environ. Mgmt.* **2007**, *14*, 298−304.

(5) Lorenzin, M. Pesticide residues in Italian ready-meals and dietary intake estimation. *J. Environ. Sci. Health, Part B* **2007**, *42*, 823−833.

(6) Nag, S. K.; Raikwar, M. K. Persistent organochlorine pesticide residues in animal feed. *Environ. Monit. Assess.* **2011**, *174*, 327−335.

(7) Witczak, A.; Abdel-Gawad, H. Assessment of health risk from organochlo-rine pesticides residues in high-fat spreadable foods produced in Poland. *J. Environ. Sci. Health, Part B* **2014**, *49*, 917−928.

(8) Chourasiya, S.; Khillare, P. S.; Jyethi, D. S. Health risk assessment of organochlo-rine pesticide exposure through dietary intake of vegetables grown in the periurban sites of Delhi, India. *Environ. Sci. Pollut. Res. Int.* **2015**, *22*, 5793−5806.

(9) Aktar, W.; Sengupta, D.; Chowdhury, A. Impact of pesticides use in agriculture: their benefits and hazards. *Interdiscip. Toxicol.* **2009**, *2* (1), 1−12.

(10) Silva, V.; Mol, H. G. J.; Zomer, P.; Tienstra, M.; Ritsema, C. J.; Geissen, V. Pesticide residues in European agricultural soils - A hidden reality unfolded. *Sci. Total Environ.* **2019**, *653*, 1532−1545.

(11) Berlett, B. S.; Stadtman, E. R. Protein oxidation in aging, disease, and oxidative stress. *J. Biol. Chem.* **1997**, *272* (33), 20313−20316.

(12) Cabras, P.; Angioni, A. Pesticide residues in grapes, wine, and their processing products. *J. Agric. Food Chem.* **2000**, *48*, 967−973.

(13) Carbajal-López, Y.; Gómez-Arroyo, S.; Villalobos-Pietrini, R.; Calderón-Segura, M. E.; Martínez-Arroyo, A. Biomonitoring of agricultural workers exposed to pesticide mixtures in Guerrero state, Mexico, with comet assay and micronucleus test. *Environ. Sci. Pollut. Res. Int.* **2016**, *23* (3), 2513−2520.

(14) Dereumeaux, C.; Mercier, F.; Soulard, P.; Hulin, M.; Oleko, A.; Pecheux, M.; Fillol, C.; Denys, S.; Quenel, P. Identification of pesticides exposure biomarkers for residents living close to vineyards in France. *Environnement International.* **2022**, *159*, 107013.

(15) Tsatsakis, A.; Tyshko, N. V.; Docea, A. O.; Shestakova, S. I.; Sidorova, Y. S.; Petrov, N. A.; Zlatian, O.; Mach, M.; Hartung, T.; Tutelyan, V. A. The effect of chronic vitamin deficiency and long term very low dose exposure to 6 pesticides mixture on neurological outcomes-A real-life risk simulation approach. *Toxicol. Lett.* **2019**, *315*, 96−106.

(16) Koutros, S.; Alavanja, M. C. R.; Lubin, J. H.; Sandler, D. P.; Hoppin, J. A.; Lynch, C. F.; Knott, C.; Blair, A.; Freeman, L. E. B. An update of cancer incidence in the Agricultural Health Study. *J. Occup. Environ. Med.* **2010**, *52* (11), 1098−1105.

(17) Pluth, T. B.; Zanini, L. A. G.; Battisti, I. D. E. Pesticide exposure and cancer: an integrative literature review. *Saúde em Debate* **2019**, *43*, 906−924.

(18) Alewu, B.; Nosiri, C. Pesticides in the Modern World—Effects of Pesticides Exposure. *Pesticides and Human Health*; Stoytcheva, M., Ed.; InTech, 2011; p 231−250. Available from: http://www.intechopen.com/books/pesticides-in-the-modern-world-effects-of-pesticides-exposure/pesticide-and-human-health.

(19) Mostafalou, S.; Abdollahi, M. Pesticides and human chronic diseases: evidences, mechanisms, and perspectives. *Toxicol. Appl. Pharmacol.* **2013**, *268*, 157−177.

(20) Kortenkamp, A. Ten years of mixing cocktails: a review of combination effects of endocrine-disrupting chemicals. *Environ. Health Perspect.* **2007**, *115*, 98−105.

(21) Katsuda, Y. Progress and future of pyrethroids. *Top. Curr. Chem.* **2011**, *314*, 1−30.

(22) Stivaktakis, P. D.; Kavvalakis, M. P.; Tzatzarakis, M. N.; Alegakis, A. K.; Panagiotakis, M. N.; Fragkiadaki, P.; Vakonaki, E.; Ozcagli, E.; Hayes, W. A.; Rakitskii, V. N.; et al. Long-term exposure of rabbits to imidaclorpid as quantified in blood induces genotoxic effect. *Chemosphere* **2016**, *149*, 108−113.

(23) Wang, Y.; Chen, C.; Qian, Y.; Zhao, X.; Wang, Q.; Kong, X. Toxicity of mixtures of λ-cyhalothrin, imidacloprid and cadmium on the earthworm Eisenia fetida by combination index (CI)-isobologram method. *Ecotoxicol. Environ. Saf.* **2015**, *111*, 242−247.

(24) World Health Organization. World Health Organization & United Nations Environment Programme. *Public Health Impact of Pesticides Used in Agriculture*; World Health Organization: Geneva, 1990; p 88. Available from: https://apps.who.int/iris/handle/10665/39772.

(25) Igbedioh, S. O. Effects of agricultural pesticides on humans, animals and higher plants in developing countries. *Arch. Environ. Health* **1991**, *46* (4), 218−224.

(26) ATSDR (Agency for Toxic Substances and Disease Registry). *Toxicological profile for pyrethrins and pyrethroids. Department of Health and Human Services*; Public Health Service Agency for Toxic Substances and Disease Registry [Internet]: Atlanta: USA, 2003. Available from: https://wwwn.cdc.gov/TSP/ToxProfiles/ToxProfiles.aspx?id=787&tid=153.

(27) Kagabu, S. Encyclopedia of Agrochemicals. In *Imidacloprid*; Plimmer Jack, R., Ed.; Wiley, 2004; pp 933−944.

(28) Katić, A.; Kašuba, V.; Kopjar, N.; Lovaković, B. T.; Marjanović Čermak, A. M.; Mendaš, G.; Micek, V.; Milić, M.; Pavičić, I.; Pizent, A.; et al. Effects of low-level imidacloprid oral exposure on cholinesterase activity, oxidative stress responses, and primary DNA damage in the blood and brain of male Wistar rats. *Chem. Biol. Interact.* **2021**, *338*, 109287.

(29) Oliver, C. J.; Softley, S.; Williamson, S. M.; Stevenson, P. C.; Wright, G. A. Pyrethroids and Nectar Toxins Have Subtle Effects on the Motor Function, Grooming and Wing Fanning Behaviour of Honeybees (Apis mellifera). *PLoS One* **2015**, *10* (8), No. e0133733.

(30) Stivaktakis, P.; Kavvalakis, M.; Goutzourelas, N.; Stagos, D.; Tzatzarakis, M.; Kyriakakis, M.; Rezaee, R.; Kouretas, D.; Hayes, W.; Tsatsakis, A. Evaluation of oxidative stress in long-term exposed rabbits to subtoxic levels of imidacloprid. *Toxicol. Lett.* **2014**, *229*, S228.

(31) Martelli, F.; Zhongyuan, Z.; Wang, J.; Wong, C. O.; Karagas, N. E.; Roessner, U.; Rupasinghe, T.; Venkatachalam, K.; Perry, T.; Bellen, H. J.; et al. Low doses of the neonicotinoid insecticide imidacloprid induce ROS triggering neurological and metabolic

https://doi.org/10.1021/acs.jproteome.3c00484
J. Proteome Res. 2023, 22, 3811−3832

impairments in *Drosophila*. *Proc. Natl. Acad. Sci. U.S.A.* **2020**, *117* (41), 25840−25850.
(32) Bonmatin, J. M.; Moineau, I.; Charvet, R.; et al. Behaviour of Imidacloprid in Fields. In *Toxicity for Honey Bees*; Lichtfouse, E., Schwarzbauer, J., Robert, D., Eds.; Environmental Chemistry: Springer. Berlin, Heidelberg (UK), 2005.
(33) Tomizawa, M.; Casida, J. E. Selective toxicity of neonicotinoids attributable to specificity of insect and mammalian nicotinic receptors. *Annu. Rev. Entomol.* **2003**, *48*, 339−364.
(34) Özdemir, S.; Altun, S.; Arslan, H. Imidacloprid exposure cause the histopathological changes, activation of TNF-α, iNOS, 8-OHdG biomarkers, and alteration of caspase 3, iNOS, CYP1A, MT1 gene expression levels in common carp (Cyprinus carpio L.). *Toxicol Rep* **2018**, *5*, 125−133.
(35) Houndji, M. A. B.; Imorou Toko, I.; Guedegba, L.; Yacouto, E.; Agbohessi, P. T.; Mandiki, S. N. M.; Scippo, M. L.; Kestemont, P. Joint toxicity of two phytosanitary molecules, lambda-cyhalothrin and acetamiprid, on African catfish (Clarias gariepinus) juveniles. *J. Environ. Sci. Health, Part B* **2020**, *55* (7), 669−676.
(36) Lonare, M.; Kumar, M.; Raut, S.; Badgujar, P.; Doltade, S.; Telang, A. Evaluation of imidacloprid-induced neurotoxicity in male rats: A protective effect of curcumin. *Neurochem. Int.* **2014**, *78*, 122−129.
(37) Fetoui, H.; Garoui, E. M.; Makni-ayadi, F.; Zeghal, N. Oxidative stress induced by lambda-cyhalothrin (LTC) in rat erythrocytes and brain: Attenuation by vitamin C. *Environ. Toxicol. Pharmacol.* **2008**, *26* (2), 225−231.
(38) Shafer, T. J.; Meyer, D. A.; Crofton, K. M. Developmental neurotoxicity of pyre-throid insecticides: critical review and future research needs. *Environ. Health Perspect.* **2005**, *113*, 123−136.
(39) Syed, F.; John, P. J.; Soni, I. Neurodevelopmental consequences of gestational and lactational exposure to pyrethroids in rats. *Environ. Toxicol.* **2016**, *31* (12), 1761−1770.
(40) Wright, G. A.; Softley, S.; Earnshaw, H. Low doses of neonicotinoid pesticides in food rewards impair short-term olfactory memory in foraging-age honey-bees. *Sci. Rep.* **2015**, *5*, 15322.
(41) Mnif, W.; Hassine, A. I. H.; Bouaziz, A.; Bartegi, A.; Thomas, O.; Roig, B. Effect of endocrine disruptor pesticides: a review. *Int. J. Environ. Res. Public Health* **2011**, *8*, 2265−2303.
(42) Jaensson, A.; Scott, A. P.; Moore, A.; Kylin, H.; Olsén, K. H. Effects of a pyrethroid pesticide on endocrine responses to female odours and reproductive behaviour in male parr of brown trout (Salmo trutta L.). *Aquat. Toxicol.* **2007**, *81*, 1−9.
(43) El-Demerdash, F. M. Lambda-cyhalothrin-induced changes in oxidative stress biomarkers in rabbit erythrocytes and alleviation effect of some antioxidants. *Toxicol. Vitro* **2007**, *21* (3), 392−397.
(44) Marsillach, J.; Costa, L. G.; Furlong, C. E. Protein adducts as biomarkers of exposure to organophosphorus compounds. *Toxicology* **2013**, *307* (307), 46−54. May
(45) Madian, A. G.; Regnier, F. E. Proteomic identification of carbonylated proteins and their oxidation sites. *J. Proteome Res.* **2010**, *9* (8), 3766−3780.
(46) Yang, X.; Bartlett, M. G. Identification of protein adduction using mass spectrometry: Protein adducts as biomarkers and predictors of toxicity mechanisms. *Rapid Commun. Mass Spectrom.* **2016**, *30* (5), 652−664.
(47) Tebourbi, O.; Sakly, M.; Rhouma, K. B. Molecular mechanisms of pesticide toxicity *Pesticides in the Modern World-Pests Control and Pesticides Exposure and Toxicity Assessment*; IntechOpen: London, UK, 2011. http://www.researchgate.net/(accessed May 30, 2014).
(48) Doganlar, Z. B.; Doganlar, O.; Tozkir, H.; Gökalp, F. D.; Doğan, A.; Yamaç, F.; Aşkın, O. O.; Aktaş, Ü. E. Nonoccupational exposure of agricultural area residents to pesticides: pesticide accumulation and evaluation of genotoxicity. *Arch. Environ. Contam. Toxicol.* **2018**, *75*, 530−544.
(49) Abdel-Halim, K. Y.; Osman, S. R. Cytotoxicity and Oxidative Stress Responses of Imidacloprid and Glyphosate in Human Prostate Epithelial WPM-Y.1 Cell Line. *J. Toxicol.* **2020**, *2020*, 1−12.
(50) Lee, H. S.; Namkoong, K.; Kim, D. H.; Kim, K. J.; Cheong, Y. H.; Kim, S. S.; Lee, W. B.; Kim, K. Y. Hydrogen peroxide-induced alterations of tight junction proteins in bovine brain microvascular endothelial cells. *Microvasc. Res.* **2004**, *68* (3), 231−238.
(51) Hashimoto, K.; Oshima, T.; Tomita, T.; Kim, Y.; Matsumoto, T.; Joh, T.; Miwa, H. Oxidative stress induces gastric epithelial permeability through claudin-3. *Biochem. Biophys. Res. Commun.* **2008**, *376* (1), 154−157.
(52) Subbarao Sreedhar, A.; Kalmár, É.; Csermely, P.; Shen, Y. F. Hsp90 isoforms: functions, expression and clinical importance. *FEBS Lett.* **2004**, *562* (1−3), 11−15.
(53) García-García, C. R.; Parron, T.; Requena, M.; Alarcón, R.; Tsatsakis, A. M.; Hernández, A. F. Occupational pesticide exposure and adverse health effects at the clinical, hematological and biochemical level. *Life Sci.* **2016**, *145*, 274−283.
(54) Stadtman, E. R. Protein oxidation and aging. *Science* **1992**, *257*, 1220−1224.
(55) Shen, L.; Chen, C.; Yang, A.; Chen, Y.; Liu, Q.; Ni, J. Redox proteomics identification of specifically carbonylated proteins in the hippocampi of triple transgenic Alzheimer's disease mice at its earliest pathological stage. *J. Proteonomics* **2015**, *123*, 101−113.
(56) Hwang, N. R.; Yim, S. H.; Kim, Y. M.; Jeong, J.; Song, E.; Lee, Y.; Lee, J.; Choi, S.; Lee, K. J. Oxidative modifications of glyceraldehyde-3-phosphate dehydrogenase play a key role in its multiple cellular functions. *Biochem. J.* **2009**, *423* (2), 253−264.
(57) Li, X. H.; Li, C.; Xiao, Z. Q. Proteomics for identifying mechanisms and biomarkers of drug resistance in cancer. *J. Proteonomics* **2011**, *74* (12), 2642−2649.
(58) Verrastro, I.; Pasha, S.; Jensen, K. T.; Pitt, A.; Spickett, C. Mass spectrometry-based methods for identifying oxidized proteins in disease: advances and challenges. *Biomolecules* **2015**, *5* (2), 378−411.
(59) Moss, S. E.; Morgan, R. O. The annexins. *Genome Biol.* **2004**, *5*, 219.
(60) The Human Protein Atlas (version.22). 2022 July 12 available from: https://www.proteinatlas.org/.
(61) Bhattacharyya, M.; Karandur, D.; Kuriyan, J. Structural Insights into the Regulation of Ca2+/Calmodulin-Dependent Protein Kinase II (CaMKII). *Cold Spring Harbor Perspect. Biol.* **2020**, *12* (6), a035147.
(62) Vinci, M.; Gowan, S.; Boxall, F.; Patterson, L.; Zimmermann, M.; Court, W.; Lomas, C.; Mendiola, M.; Hardisson, D.; Eccles, S. A. Advances in establishment and analysis of three-dimensional tumor spheroid-based functional assays for target validation and drug evaluation. *BMC Biol.* **2012**, *10* (1), 29.
(63) Zanoni, M.; Piccinini, F.; Arienti, C.; Zamagni, A.; Santi, S.; Polico, R.; Bevilacqua, A.; Tesei, A. 3D tumor spheroid models for in vitro therapeutic screening: a systematic approach to enhance the biological relevance of data obtained. *Sci. Rep.* **2016**, *6*, 19103.
(64) Preston, G. W.; Phillips, D. H. Protein Adductomics: Analytical Developments and Applications in Human Biomonitoring. *Toxics* **2019**, *7* (2), 29. May 25
(65) Wild, C. P. The exposome: From concept to utility. *Int. J. Epidemiol.* **2012**, *41*, 24−32.
(66) Roper, S. J.; Coyle, B. Establishing an *In Vitro* 3D Spheroid Model to Study Medulloblastoma Drug Response and Tumor Dissemination. *Curr. Protoc.* **2022**, *2* (1), No. e357.
(67) Collins, A. T.; Berry, P. A.; Hyde, C.; Stower, M. J.; Maitland, N. J. Prospective identification of tumorigenic prostate cancer stem cells. *Cancer Res.* **2005**, *65*, 10946−10951.
(68) Richardson, G. D.; Robson, C. N.; Lang, S. H.; Neal, D. E.; Maitland, N. J.; Collins, A. T. CD133, a novel marker for human prostatic epithelial stem cells. *J. Cell Sci.* **2004**, *117*, 3539−3545.
(69) Rizzo, S.; Attard, G.; Hudson, D. L. Prostate epithelial stem cells. *Cell Prolif.* **2005**, *38*, 363−374.
(70) O'Brien, C. A.; Pollett, A.; Gallinger, S.; Dick, J. E. A human colon cancer cell capable of initiating tumour growth in immunodeficient mice. *Nature* **2007**, *445*, 106−110.
(71) Ghosh, N.; Matsui, W. Cancer stem cells in multiple myeloma. *Cancer Lett.* **2009**, *277* (1), 1−7. May 8

https://doi.org/10.1021/acs.jproteome.3c00484
J. Proteome Res. 2023, 22, 3811−3832

(72) Schatton, T.; Murphy, G. F.; Frank, N.; Yamaura, K.; Waaga-Gasser, A. M.; Gasser, M.; Zhan, Q.; Jordan, S.; Duncan, L. M.; Weishaupt, C.; et al. Identification of cells initiating human melanomas. *Nature* **2008**, *451*, 345−349.
(73) Bertolini, G.; Roz, L.; Perego, P.; Tortoreto, M.; Fontanella, E.; Gatti, L.; Pratesi, G.; Fabbri, A.; Andriani, F.; Tinelli, S.; et al. Highly tumorigenic lung cancer CD133 $^{+}$ cells display stem-like features and are spared by cisplatin treatment. *Proc. Natl. Acad. Sci. U.S.A.* **2009**, *106*, 16281−16286.
(74) Xu, Q.; Yuan, X.; Tunici, P.; Liu, G.; Fan, X.; Xu, M.; Hu, J.; Hwang, J. Y.; Farkas, D. L.; Black, K. L.; et al. Isolation of tumour stem-like cells from benign tumours. *Br. J. Cancer* **2009**, *101*, 303−311.
(75) Hueng, D. Y.; Sytwu, H. K.; Huang, S. M.; Chang, C.; Ma, H. I. Isolation and characterization of tumor stem-like cells from human meningiomas. *J. Neurooncol.* **2011**, *104*, 45−53.
(76) Friedrich, J.; Seidel, C.; Ebner, R.; Kunz-Schughart, L. A. Spheroid-based drug screen: considerations and practical approach. *Nat. Protoc.* **2009**, *4* (3), 309−324.
(77) Vinci, M.; Gowan, S.; Boxall, F.; Patterson, L.; Zimmermann, M.; Court, W.; Lomas, C.; Mendiola, M.; Hardisson, D.; Eccles, S. A. Advances in establishment and analysis of three-dimensional tumor spheroid-based functional assays for target validation and drug evaluation. *BMC Biol.* **2012**, *10*, 29.
(78) Lee, J.; Kotliarova, S.; Kotliarov, Y.; Li, A.; Su, Q.; Donin, N. M.; Pastorino, S.; Purow, B. W.; Christopher, N.; Zhang, W.; et al. Tumor stem cells derived from glioblastomas cultured in bFGF and EGF more closely mirror the phenotype and genotype of primary tumors than do serum-cultured cell lines. *Cancer Cell* **2006**, *9* (5), 391−403.
(79) Zanoni, M.; Piccinini, F.; Arienti, C.; Zamagni, A.; Santi, S.; Polico, R.; Bevilacqua, A.; Tesei, A. 3D tumor spheroid models for in vitro therapeutic screening: a systematic approach to enhance the biological relevance of data obtained. *Sci. Rep.* **2016**, *6*, 19103.
(80) Jacob, F.; Salinas, R. D.; Zhang, D. Y.; Nguyen, P. T.; Schnoll, J. G.; Wong, S. Z. H.; Thokala, R.; Sheikh, S.; Saxena, D.; Prokop, S.; et al. A Patient-Derived Glioblastoma Organoid Model and Biobank Recapitulates Inter- and Intra-tumoral Heterogeneity. *Cell* **2020**, *180* (1), 188−204.e22. e22
(81) Chedik, L.; Bruyere, A.; Le Vee, M.; Stieger, B.; Denizot, C.; Parmentier, Y.; Potin, S.; Fardel, O. Inhibition of Human Drug Transporter Activities by the Pyrethroid Pesticides Allethrin and Tetramethrin. *PLoS One* **2017**, *12* (1), No. e0169480.
(82) Alvim, T. T.; Martinez, C. B. D. R. Genotoxic and oxidative damage in the freshwater teleost Prochilodus lineatus exposed to the insecticides lambda-cyhalothrin and imidacloprid alone and in combination. *Mutat. Res. Genet. Toxicol. Environ. Mutagen* **2019**, *842*, 85−93.
(83) Cang, T.; Dai, D.; Yang, G.; Yu, Y.; Lv, L.; Cai, L.; Wang, Q.; Wang, Y. Combined toxicity of imidacloprid and three insecticides to the earthworm, Eisenia fetida (Annelida, Oligochaeta). *Environ. Sci. Pollut. Res. Int.* **2017**, *24* (9), 8722−8730.
(84) Environmental Protection Agency (EPA). Imidacloprid: Pesticide Tolerances for Emergency Exemptions. *Federal Register*; EPA, 2005; Vol. *70* (196), pp 59268−59276. https://www.federalregister.gov/d/05-20209.
(85) European Food Safety Authority. Conclusion on the peer review of the pesticide risk assessment of the active substance lambda-cyhalothrin. *EFSA J.* **2014**, *12* (5), 3677.
(86) European Medecine Agency (EMA). Committee for Medicinal Products for Veterinary Use. European public MRL assessment report (EPMAR): Imidacloprid (fin fish). Commission Implementing Regulation (EU) No 2021/621, O.J. L 131. [Internet]. Amsterdam: The Netherlands; [Cited 2021 April 16]. 2021, available from: https://www.ema.europa.eu/en/documents/mrl-report/imidacloprid-fin-fish-summary-report-committee-veterinary-medicinal-products_en.pdf.
(87) Scheduling delegate's interim decisions and invitation for further comment: ACCS/ACMS. 3.4 Lambda-cyhalothrin. Australian Government: Department of Health and medical care. Australia. 2017 Sept 15, 2017, available from: https://www.tga.gov.au/resources/publication/scheduling-decisions-interim/scheduling-delegates-interim-decisions-and-invitation-further-comment-accsacms-march-and-july-2017.
(88) Carlsson, H.; Rappaport, S. M.; Törnqvist, M. Protein Adductomics: Methodologies for Untargeted Screening of Adducts to Serum Albumin and Hemoglobin in Human Blood Samples. *High Throughput* **2019**, *8* (1), 6. Mar 8
(89) Jeong, K.; Kim, S.; Pevzner, P. A. UniNovo: A universal tool for *de novo* peptide sequencing. *Bioinformatics* **2013**, *29*, 1953−1962.
(90) Verrastro, I.; Pasha, S.; Jensen, K. T.; Pitt, A. R.; Spickett, C. M. Mass spectrometry-based methods for identifying oxidized proteins in disease: advances and challenges. *Biomolecules* **2015**, *5* (2), 378−411. Apr 14
(91) Prianichnikov, N.; Koch, H.; Koch, S.; Lubeck, M.; Heilig, R.; Brehmer, S.; Fischer, R.; Cox, J. MaxQuant Software for Ion Mobility Enhanced Shotgun Proteomics. *Mol. Cell. Proteomics* **2020**, *19* (6), 1058−1069. Jun
(92) Unimod. 2019, [(accessed on Feb 26, 2019)] available online: http://www.unimod.org/modifications_list.php.
(93) ChemCalc Molecular Formula Finder. 2019. [(accessed on 26 February 2019)] available online: http://www.chemcalc.org/mf_finder.
(94) Molecular Weight Search. [(accessed on 26 February 2019)] available online: http://webbook.nist.gov/chemistry/mw-ser.html.
(95) Carlsson, H.; Rappaport, S. M.; Törnqvist, M. Protein Adductomics: Methodologies for Untargeted Screening of Adducts to Serum Albumin and Hemoglobin in Human Blood Samples. *High Throughput* **2019**, *8* (1), 6. Mar 8
(96) Ojha, A.; Gupta, Y. K. Study of commonly used organophosphate pesticides that induced oxidative stress and apoptosis in peripheral blood lymphocytes of rats. *Hum. Exp. Toxicol.* **2017**, *36* (11), 1158−1168.
(97) Yang, Y.; Zong, M.; Xu, W.; Zhang, Y.; Wang, B.; Yang, M.; Tao, L. Natural pyrethrins induces apoptosis in human hepatocyte cells via Bax- and Bcl-2-mediated mitochondrial pathway. *Chem. Biol. Interact.* **2017**, *262*, 38−45.
(98) Silva, A. M.; Martins-Gomes, C.; Silva, T. L.; Coutinho, T. E.; Souto, E. B.; Andreani, T. In Vitro Assessment of Pesticides Toxicity and Data Correlation with Pesticides Physicochemical Properties for Prediction of Toxicity in Gastrointestinal and Skin Contact Exposure. *Toxics* **2022**, *10* (7), 378.
(99) Weber, D.; Davies, M. J.; Grune, T. Determination of protein carbonyls in plasma, cell extracts, tissue homogenates, isolated proteins: focus on sample preparation and derivatization conditions. *Redox Biol.* **2015**, *5*, 367−380.
(100) Halliwell, B. Free radicals, antioxidants, and human disease: curiosity, cause or consequence? *Lancet* **1994**, *344*, 721−724.
(101) Dizdaroglu, M. Chemistry of free radical damage to DNA and nucleoprotein. *DNA and Free Radicals*; Halliwell, B., Aruomao, I., Eds.; Ellis Harwood: Chichester, 1993; p 19.
(102) Butterfield, D. A.; Kanski, J. Brain protein oxidation in age-related neurodegenerative disorders that are associated with aggregated proteins. *Mech Aging Dev.* **2001**, *122* (9), 945−962.
(103) Clark, J. M.; Symington, S. B. Advances in the mode of action of pyrethroids. *Top. Curr. Chem.* **2011**, *314*, 49−72.
(104) Soderlund, D. M.; Bloomquist, J. R. Neurotoxic actions of pyrethroid insecticides. *Annu. Rev. Entomol.* **1989**, *34*, 77−96.
(105) Crofton, K. M.; Reiter, L. W. Pyrethroid insecticides and the gamma-aminobutyric acidA receptor complex: motor activity and the acoustic startle response in the rat. *J. Pharmacol. Exp. Ther.* **1987**, *243* (3), 946−954. Dec
(106) Du, G.; Shen, O.; Sun, H.; Fei, J.; Lu, C.; Song, L.; Xia, Y.; Wang, S.; Wang, X. Assessing hormone receptor activities of pyrethroid insecticides and their metabolites in reporter gene assays. *Toxicol. Sci.* **2010**, *116* (1), 58−66.
(107) Sule, R. O.; Condon, L.; Gomes, A. V. A Common Feature of Pesticides: Oxidative Stress-The Role of Oxidative Stress in Pesticide-

https://doi.org/10.1021/acs.jproteome.3c00484
J. Proteome Res. 2023, 22, 3811−3832

Induced Toxicity. *Oxid. Med. Cell. Longev.* **2022**, *2022*, 1−31. ID 5563759
(108) Aouey, B.; Fares, E.; Chtourou, Y.; Bouchard, M.; Fetoui, H. Lambda-cyhalothrin exposure alters purine nucleotide hydrolysis and nucleotidase gene expression pattern in platelets and liver of rats. *Chem. Biol. Interact.* **2019**, *311*, 108796.
(109) Koshlukova, S. E. *Imidacloprid risk characterization document dietary and drinking water exposure. Health Assessment Section; Medical Toxicology Branch; Department of Pesticide Regulation*; California Environmental Protection Agency: USA, 2006 Feb 9, 2006 available from: https://www.cdpr.ca.gov/docs/risk/rcd/imidacloprid.pdf.
(110) Sheikh, M. H.; Solito, E. Annexin A1: Uncovering the Many Talents of an Old Protein. *Int. J. Mol. Sci.* **2018**, *19* (4), 1045. Mar 31
(111) Liu, Y. F.; Zhang, P. F.; Li, M. Y.; Li, Q. Q.; Chen, Z. C. Identification of annexin A1 as a proinvasive and prognostic factor for lung adenocarcinoma. *Clin. Exp. Metastasis* **2011**, *28* (5), 413−425. Jun
(112) Biaoxue, R.; Xiling, J.; Shuanying, Y.; Wei, Z.; Xiguang, C.; Jinsui, W.; Min, Z. Upregulation of Hsp90-beta and annexin A1 correlates with poor survival and lymphatic metastasis in lung cancer patients. *J. Exp. Clin. Cancer Res.* **2012**, *31* (1), 70. Aug 28
(113) Roth, U.; Razawi, H.; Hommer, J.; Engelmann, K.; Schwientek, T.; Müller, S.; Baldus, S. E.; Patsos, G.; Corfield, A. P.; Paraskeva, C.; et al. Differential expression proteomics of human colorectal cancer based on a syngeneic cellular model for the progression of adenoma to carcinoma. *Proteomics* **2010**, *10* (2), 194−202.
(114) Lecona, E.; Barrasa, J. I.; Olmo, N.; Llorente, B.; Turnay, J.; Lizarbe, M. A. Upregulation of annexin A1 expression by butyrate in human colon adenocarcinoma cells: Role of p53, NF-Y, and p38 mitogen-activated protein kinase. *Mol. Cell. Biol.* **2008**, *28* (15), 4665−4674. Aug
(115) Duncan, R.; Carpenter, B.; Main, L. C.; Telfer, C.; Murray, G. I. Characterisation and protein expression profiling of annexins in colorectal cancer. *Br. J. Cancer* **2008**, *98* (2), 426−433. Jan 29
(116) Suo, A.; Zhang, M.; Yao, Y.; Zhang, L.; Huang, C.; Nan, K.; Zhang, W. Proteome analysis of the effects of sorafenib on human hepatocellular carcinoma cell line HepG2. *Med. Oncol.* **2012**, *29* (3), 1827−1836. Sep
(117) Rondepierre, F.; Bouchon, B.; Papon, J.; Bonnet-Duquennoy, M.; Kintossou, R.; Moins, N.; Maublant, J.; Madelmont, J. C.; D'Incan, M.; Degoul, F. Proteomic studies of B16 lines: Involvement of Annexin A1 in melanoma dissemination. *Biochim. Biophys. Acta* **2009**, *1794* (1), 61−69. Jan
(118) Bai, X. F.; Ni, X. G.; Zhao, P.; Liu, S. M.; Wang, H. X.; Guo, B.; Zhou, L. P.; Liu, F.; Zhang, J. S.; Wang, K.; et al. Overexpression of annexin 1 in pancreatic cancer and its clinical significance. *World J. Gastroenterol.* **2004**, *10* (10), 1466−1470. May 15
(119) Louati, K.; Maalej, A.; Kolsi, F.; Kallel, R.; Gdoura, Y.; Borni, M.; Hakim, L. S.; Zribi, R.; Choura, S.; Sayadi, S.; Chamkha, M.; Mnif, B.; Khemakhem, Z.; Boudawara, T. S.; Boudawara, M. Z.; Safta, F. Differential Proteome Profiling Analysis under Pesticide Stress by the Use of a Nano-UHPLC-MS/MS Untargeted Proteomic-Based Approach on a 3D-Developed Neurospheroid Model: Identification of Protein Interactions, Prognostic Biomarkers, and Potential Therapeutic Targets in Human IDH Mutant High-Grade Gliomas. *J. Proteome Res.* **2023**. Aug 31
(120) Chen, R.; Chen, C.; Han, N.; Guo, W.; Deng, H.; Wang, Y.; Ding, Y.; Zhang, M. Annexin-1 is an oncogene in glioblastoma and causes tumour immune escape through the indirect upregulation of interleukin-8. *J. Cell. Mol. Med.* **2022**, *26* (15), 4343−4356. Aug
(121) Kang, J. S.; Mohler, J. L.; Ornstein, D. K.; Calvo, B. F.; Caskey, L. S.; Maygarden, S. J.; Calvo, B. F.; Maygarden, S. J.; Caskey, L. S.; Mohler, J. L.; et al. Dysregulation of annexin I protein expression in high-grade prostatic intraepithelial neoplasia and prostate cancer. *Clin. Cancer Res.* **2002**, *8*, 117−123.
(122) Patton, K. T.; Chen, H. M.; Joseph, L.; Yang, X. J. Decreased annexin I expression in prostatic adenocarcinoma and in high-grade prostatic intraepithelial neoplasia. *Histopathology* **2005**, *47* (6), 597−601. Dec
(123) Paweletz, C. P.; Ornstein, D. K.; Roth, M. J.; Bichsel, V. E.; Gillespie, J. W.; Calvert, V. S.; Vocke, C. D.; Hewitt, S. M.; Duray, P. H.; Herring, J.; et al. Loss of annexin 1 correlates with early onset of tumorigenesis in esophageal and prostate carcinoma. *Cancer Res.* **2000**, *60*, 6293−6297.
(124) Xia, S. H.; Hu, L. P.; Hu, H.; Ying, W. T.; Xu, X.; Cai, Y.; Han, Y. L.; Chen, B. S.; Wei, F.; Qian, X. H.; et al. Three isoforms of annexin I are preferentially expressed in normal esophageal epithelia but down-regulated in esophageal squamous cell carcinomas. *Oncogene* **2002**, *21* (43), 6641−6648. Sep 26
(125) Moghanibashi, M.; Jazii, F. R.; Soheili, Z. S.; Zare, M.; Karkhane, A.; Parivar, K.; Mohamadynejad, P. Proteomics of a new esophageal cancer cell line established from Persian patient. *Gene* **2012**, *500* (1), 124−133. May 25
(126) Zhou, G.; Li, H.; DeCamp, D.; Chen, S.; Shu, H.; Gong, Y.; Flaig, M.; Gillespie, J. W.; Hu, N.; Taylor, P. R.; et al. 2D Differential In-gel Electrophoresis for the Identification of Esophageal Scans Cell Cancer-specific Protein Markers. *Mol. Cell. Proteomics* **2002**, *1* (2), 117−123. Feb
(127) Vishwanatha, J. K.; Salazar, E.; Gopalakrishnan, V. K. Absence of annexin I expression in B-cell non-Hodgkin's lymphomas and cell lines. *BMC Cancer* **2004**, *4*, 8. Mar 8
(128) Silistino-Souza, R.; Rodrigues-Lisoni, F. C.; Cury, P. M.; Maniglia, J. V.; Raposo, L. S.; Tajara, E. H.; Christian, H. C.; Oliani, S. M. Annexin 1: differential expression in tumor and mast cells in human larynx cancer. *Int. J. Cancer* **2007**, *120* (12), 2582−2589. Jun 15
(129) Cheng, A.-L.; Huang, W.-G.; Chen, Z.-C.; Peng, F.; Zhang, P.-F.; Li, M.-Y.; Li, F.; Li, J.-L.; Li, C.; Yi, H.; et al. Identification of novel nasopharyngeal carcinoma biomarkers by laser capture microdissection and proteomic analysis. *Clin. Cancer Res.* **2008**, *14* (2), 435−445. Jan 15
(130) Wang, Y. Y.; Zhao, R.; Zhe, H. The emerging role of CaMKII in cancer. *Oncotarget* **2015**, *6* (14), 11725−11734. May 20
(131) Villalobo, A.; Berchtold, M. W. The Role of Calmodulin in Tumor Cell Migration, Invasiveness, and Metastasis. *Int. J. Mol. Sci.* **2020**, *21* (3), 765.
(132) He, Q.; Li, Z. The dysregulated expression and functional effect of CaMK2 in cancer. *Cancer Cell Int.* **2021**, *21*, 326.
(133) Wang, J.; Xu, X.; Jia, W.; Zhao, D.; Boczek, T.; Gao, Q.; Wang, Q.; Fu, Y.; He, M.; Shi, R.; et al. Calcium-/Calmodulin-Dependent Protein Kinase II (CaMKII) Inhibition Induces Learning and Memory Impairment and Apoptosis. *Oxid. Med. Cell. Longev.* **2021**, *2021*, 1−19. ID 4635054
(134) Yokokura, S.; Yurimoto, S.; Matsuoka, A.; Imataki, O.; Dobashi, H.; Bandoh, S.; Matsunaga, T. Calmodulin antagonists induce cell cycle arrest and apoptosis in vitro and inhibit tumor growth in vivo in human multiple myeloma. *BMC Cancer* **2014**, *14*, 882.
(135) Annabi, B.; Pilorget, A.; Bousquet-Gagnon, N.; Gingras, D.; Béliveau, R. Calmodulin inhibitors trigger the proteolytic processing of membrane type-1 matrix metalloproteinase, but not its shedding in glioblastoma cells. *Biochem. J.* **2001**, *359*, 325−333.
(136) Brzozowski, J. S.; Skelding, K. A. The Multi-Functional Calcium/Calmodulin Stimulated Protein Kinase (CaMK) Family: Emerging Targets for Anti-Cancer Therapeutic Intervention. *Pharmaceuticals* **2019**, *12* (1), 8. Jan 7
(137) Hegyi, B.; Borst, J. M.; Lucena, A. J.; Bailey, L. R.; Bossuyt, J.; Bers, D. M. Diabetic Hyperglycemia Regulates Potassium Channels and Arrhythmias in the Heart *via* Autonomous CaMKII Activation by O-Linked Glycosylation. *Biophys. J.* **2019**, *116*, 98a.
(138) Toxic Exposome Database, T3DB. 2019, [(accessed on 26 February 2019)] available online: http://www.t3db.ca/.
(139) Neveu, V.; Moussy, A.; Rouaix, H.; Wedekind, R.; Pon, A.; Knox, C.; Wishart, D. S.; Scalbert, A. Exposome-Explorer: A manually-curated database on biomarkers of exposure to dietary and environmental factors. *Nucleic Acids Res.* **2017**, *45*, D979−D984.

https://doi.org/10.1021/acs.jproteome.3c00484
J. Proteome Res. 2023, 22, 3811−3832